PUBLICATIONS OF THE ASTRONOMICAL SOCIETY OF THE PACIFIC
87:37–63, 1975 February

STRUCTURE AND AGE OF THE LOCAL ASSOCIATION (PLEIADES GROUP)

O. J. EGGEN
Mount Stromlo and Siding Spring Observatory
Research School of Physical Sciences
The Australian National University

Received 1974 September 24

The available photometric and motion parameters for some 500 early-type stars brighter than $M_V = -1^m$ are used to compute space-motion vectors. It is concluded that (a) about one-third of the stars are members of the local association (Pleiades group) which are easily isolated from the other interarm stars because $V = -25$ km sec^{-1}; (b) some 50 stars with aberrant velocity vectors, and often referred to as "runaway stars", may actually be members of the old-disk, or even the halo, population; (c) perhaps the local association (or Gould Belt) stars cannot be separated from other interarm objects on the basis of positional criteria alone; and (d) the age spread in the local association ranges from that of the cluster NGC 2287 to pre-main-sequence stars in several star-producing regions within the association including the large Taurus Aurigae dark cloud and isolated small clouds, such as that near HR 5999/6000.

Key words: local association — Gould's Belt — stellar motions

I. Introduction

Strömgren indices, $(b-y)$, m_1, c_1, and β, are now available for almost all stars in the Catalogue of Bright Stars and of type A0 or earlier, mainly as a result of observations by Crawford and his associates (Crawford and Barnes 1970; Crawford, Barnes, and Golson 1970, 1971; Crawford et al. 1973; Crawford, Barnes, and Warren 1974) and by Stokes (1972*a*,*b*). The luminosities computed from these indices lead to accurate space motions for the large number of objects with well-determined proper motions and radial velocities. The present discussion is based on the space motions of 500 stars brighter than $M_V = -1^m$ and in the temperature range indicated by $[u-b] = -0^m050$ to $+1^m300$ ($\log T_e \sim 4.05$ to 4.4; Eggen 1974*b*, Table 13). Because they are few in number and generally have less reliable proper motions, the few stars with a distance modulus greater than 10^m0 have arbitrarily been eliminated.

II. Basic Data

The Strömgren indices yield the reddening free parameters β and $[u-b] = [c_1] + 2[m_1]$, where $[c_1] = c_1 - 0.20\,(b-y)$ and $[m_1] = m_1 + 0.18\,(b-y)$ (Strömgren 1966). The luminosities are computed from $M_V = f([u-b], \beta)$ by the method described elsewhere (Eggen 1974*b*,*c*). The values of $[u-b]$ will be given in units of 0^m001 throughout this paper. Three-color, photoelectric photometry is also available for these objects and the values of V_0 have been determined from $V_0 = V - 3.0\mathrm{E}\,(B-V)$, where $\mathrm{E}(B-V)$ is derived from standard $(U-B, B-V)$ relations (Eggen 1965; Cousins, Eggen, and Stoy 1961).

All proper motions are on the FK4 system with precessional corrections and are based on all available meridian observations; the compilations by Lesh (1968, 1972) were used extensively. The sources of the radial velocities are listed by Abt and Biggs (1972).

III. Associations in the Nearby Spiral Arm

In order to roughly delineate the interarm region, populated by most of the present sample of stars, a few of the nearer associations in the outer (Orion) arm are listed in Table I and shown as filled circles in Figure 1. The parameters for some of these associations are derived in Table II. The inner (Sagittarius) arm is not represented in the present data but a few of the associations that mark its outer edge are shown in Figure 1 as open circles on the basis of data published by Ruprecht (1966). The X coordinate in Figure 1 is positive away from the galactic center and Y increases in the direction of galactic rotation.

TABLE I

OB ASSOCIATIONS NEAR THE EDGE OF THE OUTER SPIRAL ARM

Ass.	V_O-M_V	U	V	W	X	Y	Z
		(km/sec)			(parsecs)		
Cyg OB 3	$11^m.1$	-	-	-	- 505	+1580	+ 65
Cyg OB 1*	10.3	-	-	-	- 390	+1076	- 75
Lac OB 1	8.1	- 5	-14	- 1	+ 54	+ 396	-116
Cep OB 3*	9.3	-35	-11	+ 1	+ 248	+ 680	+ 29
Cam OB 1	8.35	- 4	- 5	- 7	+ 368	+ 288	+ 20
Per OB 2	7.6	+22	- 7	-11	+ 300	+ 95	- 95
Aur OB 1*	10.55	-	-	-	+1276	+ 176	+ 27
Mon OB 1*	9.6	-	-	-	+ 770	- 320	+ 25
Ori OB 1	7.85	+18	-10	-12	+ 325	- 142	-110

*Cyg OB 1 Distance based on that of the cluster NGC 6913.

Cep OB 3 Distance from Crawford and Barnes (1970) and proper motion and radial velocity from Garmany (1973).

Aur OB 1 Distance from the clusters NGC 1912 ($V_O-M_V = 10^m.5$) and NGC 1960 ($V_O-M_V = 10^m.6$).

Mon OB 1 The distance is derived from the cluster NGC 2264 (e.g. Eggen 1974b).

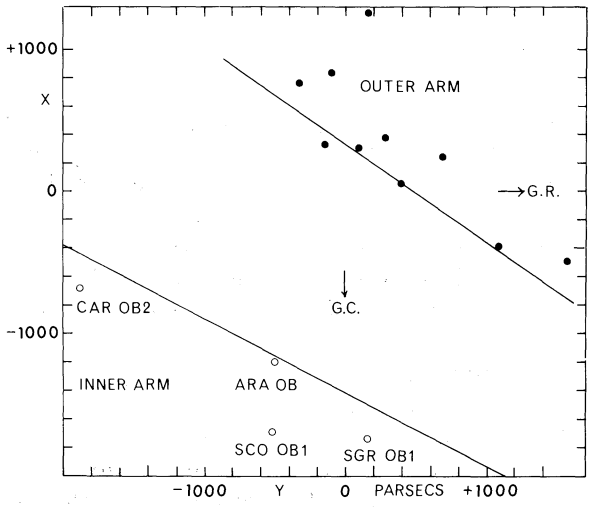

FIG. 1 — Positions in the (X,Y) plane of associations (Table I) on the boundaries of the neighboring spiral arms.

IV. The Local Association

The present sample contains the 77 members of the Pleiades group listed in Table III plus an additional 61 stars, listed in Table IV, which are discussed elsewhere (Eggen 1974*b,c*) and are not repeated here. These objects constitute the local association, which is sometimes referred to as Gould's Belt. Fortunately, the V vectors, -25 km sec^{-1} of association members are distinctive for young stars, as will be discussed in the next section, and with the accurate luminosities available from the photometric indices, they are easily isolated. A previous discussion of the stars in Table IV that have the most accurately determined radial velocities and proper motions (Eggen 1974*b*) led to a dispersion of only $0^m.3$ in the comparison of group luminosities, derived from forcing $V = -25$ km sec^{-1}, and the values found

TABLE II

INDIVIDUAL STARS IN THE OB ASSOCIATIONS OF THE OUTER SPIRAL ARM

Star	[u-b]	β	M_V	V_O	V_O-M_V	μ_α (0".001)	μ_δ (0".001)	ρ (km/sec)
Cyg OB 3 *								
2	0	2.564	-5.4	5.7	11.1	-	-	-
3	+ 15	2.563	-5.35	5.8	11.15	-	-	-
5	- 38	2.579	-4.85	6.3	11.15	-	-	-
7	+ 26	2.602	-3.7	7.4	11.1	-	-	-
8	+ 76	2.606	-3.4	7.5	10.9			
					11.1			
Lac OB 1								
HR 8427	301	2.638	-2.55	5.9	8.45	- 1	- 5	-17.8
HR 8549	323	2.569	-1.85	6.2	8.05	- 1	- 6	- 8.6
HR 8553	326	2.647	-2.3	5.85	8.15	0	- 1	-16.8
HR 8603	137	2.618	-2.75	5.35	8.1	- 4	- 4	-13.0
HR 8622	- 66	2.590	(-3.5)	4.6	(8.1)	+ 2	- 4	-14.5
HR 8640	149	2.613	-3.2	4.9	8.1	+ 1	+ 2	-14.4
HR 8651	222	2.637	-2.4	6.05	8.45	+ 2	- 8	-17.8
HR 8690	443	2.634	-2.95	5.1	8.05	+ 4	- 2	-15.3
HR 8728	417	2.661	-2.0	5.8	7.8	- 2	- 4	- 8.5
					8.1	0	- 3	-13.5
Cam OB 1								
HR 1035	+ 2	2.554	-5.6	2.95	8.55	- 1	- 4	- 6.8
HR 1040	- 8	2.568	-5.15	3.0	8.15	- 1	0	- 6.0
					8.35	- 1	- 3	- 6.4
Per OB 2								
IC 348*	-	-	-	-		+ 5	-10	-
HR 1074	123	2.623	-2.2	5.3	7.5	- 5	+ 2	+25.0
HR 1123	65	2.600	-3.65	4.2	7.85	+12	- 8	+27.1
HR 1131	121	2.597	-3.75	3.55	7.3	+10	-12	+18.0
HR 1191	110	2.620	-2.8	5.05	7.85	- 4	- 3	+17.4
HR 1203	- 2	2.564	-5.4	2.0	7.4	+ 5	- 9	+20.6
HR 1215	232	2.642	-2.45	4.9	7.35	+ 6	- 3	+17.6
					7.6	+ 4	- 8	+21.5
Gem OB 1								
HR 2084	- 13	2.565	-4.6	4.7	9.3	- 2	- 3	+ 8.0
HR 2111	531	2.588	-4.6	5.2	9.8	- 1	+ 5	+16.6
HR 2173	71	2.554	-5.45	4.3	9.75	- 3	- 5	+16.0
HR 2240	144	2.548	-5.55	4.35	9.9	0	- 3	+13.2
					9.7	- 1.5	- 1.5	+13.5
Ori OB 1								
HR 1748	308	2.639	-2.5	6.0	8.5	- 6	0	+29.0
HR 1756	21	2.603	-3.7	4.2	7.9	- 7	- 4	+20.2
HR 1763	113	2.611	-3.15	5.45	8.6	-	-	-
HR 1765	321	2.628	-2.95	4.55	7.5	- 2	- 2	+28.8
HR 1770	184	2.617	-3.0	4.65	7.65	0	+ 3	+18.0
HR 1781	209	2.638	-2.3	5.55	7.85	- 2	- 3	+22.1
HR 1786	516	2.681	-1.65	6.2	7.85	-	-	-
HR 1803	396	2.659	-2.0	6.05	8.05	-	-	-
HR 1811	172	2.632	-2.45	5.15	7.6	0	- 8	+12.2
HR 1820	406	2.669	-1.7	6.3	8.0	- 3	+ 3	+34.2
HR 1833	273	2.640	-2.4	5.65	8.05	-	-	-
HR 1848	410	2.671	-1.65	6.1	7.75	-	-	+23.0
HR 1852	- 22	2.574	-5.25	2.15	7.4	- 1	- 1	+16.0
HR 1855	12	2.598	-3.5	4.45	7.95	-	-	+17.4
HR 1861	133	2.612	-3.05	5.1	8.15	+ 2	- 1	+34.3
HR 1903	- 44	2.557	-6.0	1.5	7.5	- 3	- 2	+26.1
HR 1906	307	2.665	-1.6	6.45	8.05	- 3	- 1	-
HR 1933	249	2.636	-2.45	5.75	8.2	-	-	-
HR 1942	699	2.714	-1.05	6.35	7.4	+ 1	- 5	+21.0
HR 1952	279	2.626	-2.9	4.9	7.8	- 2	- 8	+29.7
HR 2004	- 37	2.564	-5.65	1.9	7.55	- 2	- 5	+20.6
HR 2031	265	2.647	-2.1	5.2	7.3	-	-	-
					7.85	- 2	- 2.5	+23.5

*Cyg OB 3 The star numbers are those used by Crawford et al (1974).

IC 348 The proper motion is based on data by Fredrick (1956).

TABLE III

MEMBERS OF THE LOCAL ASSOCIATION (PLEIADES GROUP)

HR	[u-b]	β	M_V	V_O	μ_α	μ_δ	ρ	U	V	W	X	Y	Z
	($0^m.001$)				($0''.001$)		(km/sec)		(km/sec)			(Parsecs)	
113	764	2.689	$-1^m.85$	$5^m.5$	+12	- 6	-19:	+ 4	-25	- 9	+151	+259	- 15
121	680	2.709	-1.65	5.95	+22	- 4	- 9.5	+24	-25	- 9	+167	+280	+ 21
422	1172	2.724	-1.3	6.45	+12	-19	- 0.7	+11	-25	-26	+213	+250	-133
944	949	2.706	-1.7	5.0	+20	-15	- 2.0	+ 8	-25	- 1	+183	+ 82	- 92
950	558	2.677	-1.2	5.85	+24	-15	+ 7.9	+24	-25	- 2	+208	+126	- 58
1113	757	2.719	-1.0	5.25	+21	-26	- 1.0	+ 8	-25	- 6	+151	+ 66	- 41
1141	686	2.702	-1.25	5.35	+24	-18	+ 2.2	+16	-25	0	+182	+ 97	- 26
1153	484	2.678	-2.2	5.05	+16	-10	+17.0	+17	-25	- 4	+229	- 5	-169
1244	644	2.708	-1.15	5.2	+23	-14	+13.5	+12	-25	0	+144	- 30	-114
1258	359	2.654	-2.4	6.3	+ 1	- 9	+20.0	- 5	-25	-18	+319	-220	-397
1512	487	2.663	-2.3	5.6	+ 3	-16	+20.7	+18	-25	-18	+370	+ 22	- 92
1520	592	2.656	-2.8	3.9	+13	-12	+23.0	+15	-25	- 6	+185	- 69	-111
1808	598	2.694	-1.3	5.2	+ 6	-25	+17.6	+13	-25	-11	+198	- 25	- 33
1875	447	2.675	-2.0	5.0	+11	-16	+22.8	+21	-25	- 1	+258	- 13	- 20
1918	182	2.618	-3.0	5.9	- 1	- 6	+30.0	+15	-25	-20	+494	-282	-158
1946*	476	2.672	-1.55	5.4	+ 5	-18	+21.1	+16	-25	- 9	+240	- 42	- 31
1993	478	2.653	-2.15	5.1	+ 1	-16	+30.0	+22	-25	-13	+272	- 64	- 36
2199	487	2.666	-2.05	4.4	+ 1	-24	+24.0	+17	-25	-10	+183	- 52	- 7
2207	792	2.719	-1.0	6.3	+ 2	-17	+21.3	+16	-25	- 8	+272	- 58	+ 2
2282*	459	2.677	-1.6	2.9	+ 9	+ 4	+31:	+17	-25	- 6	+ 40	- 63	- 26
2410*	535	2.670	-2.05	6.05	- 6	+ 6	+32.0	+13	-25	-24	- 9	-375	-183
2596	344	2.582	-4.6	3.85	- 6	0	+41.0	+30	-25	-17	+321	-365	- 57
2602	-	-	-1.55	5.35	+ 6	+19	+18.5	+16	-25	+ 2	- 44	-215	-105
2840	767	2.683	-2.25	6.3	+ 5	- 4	+28.8	+17	-25	+13	+448	-228	+114
3025	403	2.644	-2.5	6.35	- 4	+ 2	+30:	+18	-25	-11	+157	-562	- 77
3078	246	2.623	-2.95	5.9	-10	+ 3	+32.2	+24	-25	-21	+110	-490	- 70
3091	417	2.658	-2.1	5.45	- 4	- 3	+27.0	+ 8	-25	-10	+102	-306	- 23
3326	551	2.664	-2.3	5.4	- 8	+ 7	+27.8	+21	-25	- 5	+ 60	-341	- 15
3571	772	2.701	-1.4	3.4	-20	+40	+22:	+15	-25	0	+ 12	- 89	- 16
3849	597	2.700	-1.0	4.9	-30	-21	+18:	+13	-25	-15	+ 48	-124	+ 70
3858	Emission		-1.0	4.55	-29	- 1	+25.9	+19	-25	- 2	+ 29	-116	+ 47
4222	490	2.658	-2.7	4.7	-18	+ 9	+16.0	+22	-25	- 2	-105	-288	- 25
4361	313	2.606	-4.0	5.4	- 7	- 2	+18.3	+13	-25	-16	-279	-735	+ 13
4731*	-	-	-3.0	2.0	-24	-12	+22.5	0	-25	- 7	- 52	- 90	- 1
4897	526	2.681	-1.95	4.5	-26	-21	+12:	+12	-25	-18	-107	-162	+ 13
5206	362	2.634	-2.3	5.6	-17	-14	- 4.1	+25	-25	-18	-253	-266	+ 96
5210*	433	2.668	-1.8	4.45	-37	-22	+11.4	+ 5	-25	0	- 81	- 75	+ 59
5217	680	2.679	-1.4	5.35	-29	- 1	+ 7.4	+18	-25	- 7	-150	-165	+ 33
5248	272	2.628	-2.6	3.75	-27	-18	+ 4.9	+14	-25	- 7	-128	-124	+ 61
5425	208	2.625	-2.55	4.25	-27	-17	- 1.8	+23	-25	- 6	-169	-147	+ 37
5440	Emission		-3.4	2.2	-36	-32	+ 5.5	+16	-25	- 9	-104	- 79	+ 39
5595	526	2.706	-1.25	5.35	-14	-22	+ 5.6	+ 2	-25	- 8	-172	- 89	+ 80
5605*	561	2.708	-1.55	4.5	-25	-18	+10:	+ 5	-25	- 1	-130	- 90	+ 28
5651*	455	2.678	-1.35	4.75	-18	-20	+13.5	- 2	-25	- 3	-137	- 86	+ 33
5695	204	2.616	-3.75	3.1	-16	-29	+ 0.7	+10	-25	-11	-200	-110	+ 56
5778*	639	2.681	-1.85	4.0	-19	-12	-25:	+ 9	-25	-13	- 52	- 66	+120
5915	501	2.684	-1.5	5.35	-18	-13	- 6.5	+11	-25	+ 1	-227	- 33	+110

TABLE III - CONTINUED

HR	[u-b]	β	M_V	V_O	μ_α	μ_δ	ρ	U	V	W	X	Y	Z
	($0^m.001$)				($0''.001$)		(km/sec)		(km/sec)			(Parsecs)	
5948	252	2.615	$-2^m.9$	$3^m.4$	-14	-30	+ 1.1	+ 7	-25	-11	-166	- 65	+ 35
5987	426	2.668	-1.35	4.1	-20	-31	+15.1	- 6	-25	- 2	-115	- 40	+ 24
5988	600	2.721	-1.15	5.6	-10	-24	- 9.5	+ 9	-25	-14	-210	- 36	+ 81
5993	109	2.621	-3.4	3.25	-13	-23	+ 4:	+ 3	-25	- 7	-197	- 25	+ 83
6174	437	2.684	-1.55	5.3	- 9	-23	+ 1.5	+ 7	-25	-10	-222	- 79	+ 10
6214	485	2.680	-1.0	5.35	-10	-25	+10.0	- 3	-25	- 7	-182	- 55	+ 11
6320	583	2.701	-1.25	5.55	- 5	-26	+ 6.9	+ 8	-25	-14	-199	-106	- 39
6510	Emission		-1.65	2.8	-26	-70	0:	+10	-25	- 6	- 72	- 25	- 12
7074	147	2.573	-4.15	3.8	- 5	-11	+15:	- 4	-25	- 2	-319	-158	-158
7106*	Emission		-3.9	3.2	+ 4	- 3	-29.4	+11	-25	-13	-115	+227	+ 67
7129	489	2.683	-0.7	5.3	-11	-32	+ 2.0	- 1	-25	- 2	-141	- 42	- 60
7158	1000	2.703	-1.5	6.2	- 2	-15	-10.0	- 6	-25	- 9	-284	+205	- 1
7401	644	2.706	-1.25	6.55	- 7	+10	-21.0	+12	-25	+10	- 3	+344	+115
7447	746	2.711	-1.3	4.1	+ 3	-29	-22:	+10	-25	- 5	- 94	+ 71	- 22
7467	515	2.666	-2.1	6.35	+ 3	0	-28.0	+11	-25	-10	-150	+461	+ 71
7486*	598	2.704	-1.2	6.45	- 3	-13	-14.2	- 7	-25	- 5	-213	+262	- 26
7565*	454	2.667	-2.15	4.7	+27	-16	-28.0	+15	-25	-34	-118	+202	- 8
7572	732	2.658	-1.9	6.05	+ 4	-15	-12.6	- 5	-25	-18	-253	+293	- 58
7608	639	2.715	-1.0	5.05	+ 5	+10	-26.0	+ 9	-25	- 8	+ 1	+157	+ 42
7613	632	2.672	-2.25	4.7	+ 8	- 2	-28:	+10	-25	-12	- 68	+235	+ 22
7620	555	2.674	-2.0	5.95	+ 5	- 7	-23.0	+ 1	-23	-16	-119	+369	+ 26
7623	459	2.661	-2.5	4.2	+ 7	-26	+ 0.9	+ 4	-25	-13	-192	+ 19	-105
7628	605	2.679	-2.0	5.25	+ 4	- 6	-28:	+15	-25	- 3	- 69	+271	+ 29
7664	793	2.695	-1.5	5.5	+ 2	- 7	-25:	+10	-25	- 3	-141	+205	- 35
7700	454	2.680	-1.5	6.2	+ 2	+ 3	-38.2	+28	-25	+ 8	-211	+266	- 71
7852	744	2.702	-2.05	3.95	+13	-22	-19.3	+ 6	-25	-12	- 86	+125	- 45
7992	763	2.718	-0.85	6.1	+12	-22	- 4.0	+17	-25	- 7	-193	- 41	-165
8136	470	2.680	-1.55	6.3	+10	+ 1	-25:	+13	-25	-11	+ 1	+371	- 4
8215	508	2.639	-2.95	5.1	+ 2	0	-25:	+ 5	-25	0	- 42	+399	- 70
8403	680	2.697	-1.5	5.6	+ 5	+ 3	-24.0	+ 4	-25	0	+ 41	+260	- 9

Notes to Table III

1946 Close binary with equal components.

2282 Sp.B/ 675 days.

2410 Sp.B. 3.0 days.

4731 Cpm with HR 4729 and 4730. Proper motion based on mean for the three stars and radial velocity on mean for 4729 and 4731. 4730 is Sp.B. with a period of 75.8 days and a discordant value of ρ = + 7.5 km/sec.

5210 Previously (Eggen 1974b) the parameters of both components were used. The present discussion is based on the bright component alone. A single observation with the 40-inch reflector gives $(V_E, B-V, U-B) = (4^m.62, -0^m.16, -0^m.67)$.

5605AB Close binary, equal components.

5651 Sp.B. 0.9 days.

Notes to Table III - Continued

5778 θ CrB. Suspected close binary (0".5) with Δm varying from 1^m.5 to 3^m.5; larger, short period light variations in the v and b bands of the Strömgren indices have been reported (Roark 1971).

7106 β Lyr; 12.9 days. The possibility that this interesting system is a member of the group depends entirely on the adopted radial velocity which is the value derived by Abt et al. (1962) for the 4.3 day spectroscopic binary called component B. The proper motion has little effect on the V velocity so if the radial velocity is as small as -19 km/sec, the mean systemic velocity of β Lyr, the system is not a group member. The distance derived by Abt et al. is adopted here.

7486 QS Aql. Sp.B. 2.5 days. Close binary, equal components.

7565 Sp.B. 3.7 days.

TABLE IV

STARS DISCUSSED IN EGGEN 1974b (TABLE 11) AND EGGEN 1974c (TABLE II)

HR	HR	HR	HR
193	2618	4992	5885
472	2657	5190	5928
542	3129	5191	5941
548	3162	5231	5944
721	3582	5249	5967
1087	3659	5285	6165
1220	3825	5358	6247
1273	4618	5378	6252
1320	4621	5440	6743
1350	4638	5453	6870
1641	4679	5471	6897
1791	4853	5528	7029
1928	4898	5543	7147
2159	4899	5576	7750
2198	4940	5712	7790
2451			

from the photometric parameters. A similar result is obtained from the present material if we consider only the stars for which the proper motion contributes substantially to the V velocity. There are still many relatively bright, early-type stars that are candidates for group membership but which lack accurately determined radial velocities. Many of these are spectroscopic binaries and orbital elements will be necessary to fix the systemic velocities with the required accuracy.

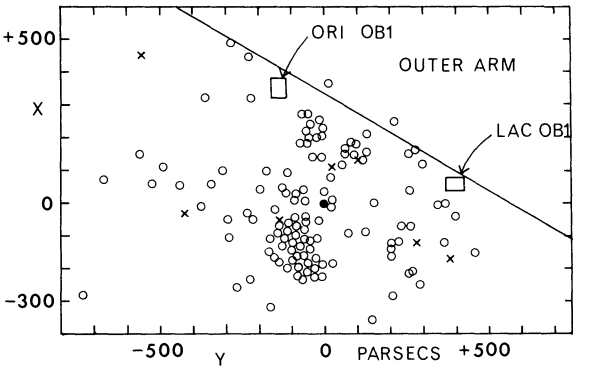

FIG. 2 — The local association (Pleiades group) members in the (X,Y) plane. The inner boundary of the Orion arm and two associations at this boundary are also indicated.

The distribution of the group stars in the (X,Y) plane is shown in Figure 2 where the location of the associations Orion OB 1 and Lacerta OB 1 are also indicated. The seven crosses represent the seven clusters (Eggen 1974*b*, Table 9) that are probably members of the group. The position of the sun is marked by a filled circle.

There are three or four major concentrations of group members in Figure 2. The largest marks what is sometimes referred to as the Scorpius-Centaurus stream, with a center near $(X, Y) = (-125, -75)$ parsecs and includes the cluster IC 2602. The small clump of stars near the Pleiades and α Persei clusters, (X,Y) near (+175,

+75), are in front of the Taurus dark cloud and a heavier concentration is elongated in the direction of the Orion association. A line of stars, some 600 parsecs long in the direction of the relatively clear, anticenter direction, and including the cluster NGC 2516, is also noticeable.

The group members are shown in the ($[u-b]$, M_V) plane of Figure 3 where the zero-age main sequence (ZAMS) and the evolved sequences of the α Per (and NGC 2602), Pleiades, and NGC 2287 clusters are also shown schematically (Eggen 1972, 1974*b*). To test for any correlation between the age and galactic position, the stars with positive values of X in Figure 2 are shown as open circles in Figure 3 and the remainder are represented by filled circles. There are no marked differences between the age distributions of these two subgroups and they probably both represent the same age spread as found for the clusters in the association. The few, very early-type stars, with $[u-b] < 200$, may be blue stragglers similar to θ Carinae in NGC 2602, with (M_V, $[u-b]$) = (-3^m2, 100) and HR 3147 in NGC 2516 with (-2^m9, 200) (Eggen 1974*b*, Fig. 6).

V. Nongroup Interarm Stars

With the exception of about 50 stars showing aberrant velocities, discussed below, the remaining stars of the sample are listed in Tables V and VI. The ten stars in Table VI are the only objects in the sample, other than the association members discussed above, that may be located in the outer spiral arm. These objects are represented by crosses in the (X, Y) plane of Figure 4 where the stars in Table V are shown as open circles. The two OB associations, Lac 1 and Ori 1 are also indicated and the position of the sun is marked by a filled circle. Three stars listed at the ends of Table VI, HR 7567, HR 7767, and HR 7977 (55 Cygni), have not been assigned to any of the many known associations in Cygnus but the very consistent modulus of 9^m6 given by these objects is the same as that found for the neighboring association Cygnus OB 7 (sometimes called XI Cyg or Cyg VI). The existence of this association, consisting of a half dozen heavily reddened stars fainter than visual magnitude 6^m5, is not well established. Schmidt-Kaler (1961) suggests that the K0 I*b* supergiant HR 8248 may also be an association member, and the parameters of this star, the last entry in Table VI, support the suggestion. These stars are shown as plus signs in Figure 4. The vectors of the mean space velocity, (U, V, W) = (-6, -7, -9) km sec^{-1}, are quite similar to those for two other associations on the edge of the outer spiral arm, Lac OB1 and Camelopardalis OB1 (see Table I).

The stars of Table V are more randomly distributed in the (X, Y) plane of Figure 4 than the group members in Figure 3 but there are a number of concentrations. Perhaps the most obvious features of Figure 4 are the marked zone of avoidance near the sun in the $-X$, $-Y$ direction, probably caused by the heavy absorption in Ophiuchus, and a 500-parsec lane in the direction of $\ell = 255°$. The latter rift in the star distribution, which is in the direction of Canis Major OB 1, is not caused by absorption because the nearly

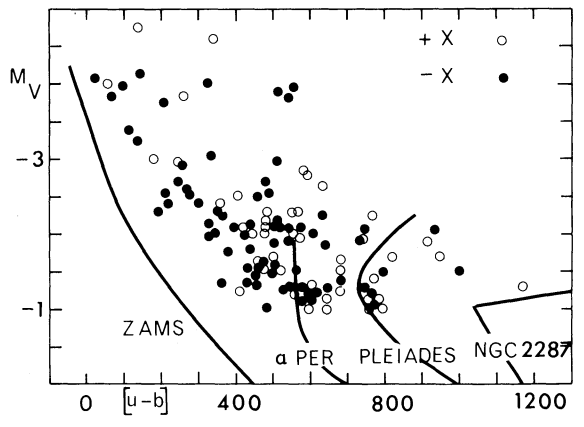

FIG. 3 — The stars of Figure 2 in the (M_V, $[u-b]$) plane. The schematic, evolved sequences of several clusters in the local association are also shown.

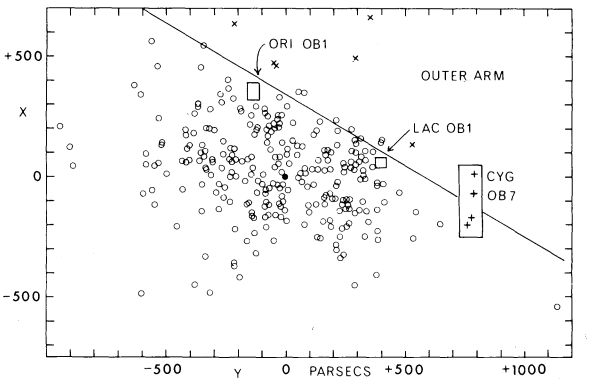

FIG. 4 — Same as Figure 2 but for interarm stars other than members of the local association (Table V).

TABLE V

OTHER INTERARM STARS

HR	[u-b] ($0^m.001$)	β	M_V	V_O	μ_α ($0''.001$)	μ_δ ($0''.001$)	ρ (km/sec)	U (km/sec)	V (km/sec)	W (km/sec)	X (Parsecs)	Y (Parsecs)	Z (Parsecs)
7	1072	2.725	$-1^m.2$	$5^m.3$	+ 7	+ 5	- 0.4	+ 6	- 4	+ 3	+ 94	+176	+ 6
38	359	2.652	-2.15	6.35	+ 3	- 2	- 9.6	+ 1	-13	- 1	+169	+414	+208
39	285	2.629	-2.8	2.8	+ 4	-12	+ 4.1	0	- 3	- 8	+ 30	+ 87	- 98
62	768	2.675	-1.95	5.7	+ 9	+ 8	- 8.5	+12	-12	+13	+150	+292	- 85
91	548	2.693	-1.35	5.4	+15	- 6	-14.5	+ 6	-21	- 5	+105	+193	- 41
153	294	2.625	-3.0	3.5	+19	- 9	+ 2.0	+15	- 8	-10	+100	+160	- 30
154*	620	2.688	-1.95	5.0	+17	- 5	+ 8.7	+19	- 6	-10	+105	+186	-120
155	465	2.695	-1.05	5.7	+ 6	- 8	- 6.3	0	-12	- 1	+ 70	+134	-165
179	531	2.656	-2.5	4.55	+14	- 3	- 4.6	+12	-13	- 3	+130	+213	- 55
208*	773	2.705	-1.3	5.2	+16	- 7	- 0.8	+13	- 8	- 7	+106	+165	- 41
302	503	2.680	-1.65	6.1	+12	- 4	- 4.2	+14	-16	- 5	+200	+284	- 72
533	248	2.650	-1.95	5.3	+11	- 8	- 9.0	+ 6	-18	- 6	+190	+214	- 34
679	642	2.688	-1.75	5.85	+13	- 3	+ 1.6	+17	-20	-20	+240	+215	- 74
779*	258	2.624	-2.95	3.95	+10	- 3	+13.0	+14	- 9	- 9	+151	+ 25	-198
801	519	2.682	-1.6	4.5	+ 8	-10	+ 7.0	+ 8	- 6	- 7	+127	+ 70	- 80
811	791	2.719	-1.0	4.2	- 9	-17	+15.4	- 1	- 5	-18	+ 53	+ 11	- 96
836*	673	2.703	-1.35	4.85	+ 6	-15	+ 8.8	+ 6	- 9	-11	+130	+ 50	-105
1059	1036	2.712	-1.4	5.8	+10	- 4	- 5.2	+ 3	-14	+ 4	+232	+146	- 27
1121	630	2.686	-1.8	5.5	- 7	- 4	+15.7	+ 4	0	-19	+202	- 43	-200
1122	690	2.671	-2.2	2.85	+26	-35	+ 2.7	+12	-17	- 6	+ 89	+ 50	- 10
1239*	559	2.679	-1.85	3.35	- 6	-11	+14.8	+10	- 2	-12	+ 93	+ 3	- 53
1253	522	2.697	-1.15	5.0	+ 3	- 9	+10.7	+ 7	- 8	- 8	+141	- 13	- 93
1288	574	2.690	-1.55	5.25	0	+ 4	+13.7	+12	- 2	- 8	+144	- 84	-157
1305	667	2.715	-1.05	5.6	+ 8	-13	0.0	+ 9	-12	- 4	+173	+122	+ 30
1312	588	2.677	-2.0	6.4	0	- 9	+20.3	+ 6	-19	-21	+381	- 92	-275
1363	708	2.704	-1.3	5.7	- 2	- 9	+11.0	+ 1	- 9	-12	+187	- 74	-151
1378*	515	2.682	-1.6	5.3	+ 4	-11	+15.0	+14	-11	- 9	+227	+ 29	- 72
1397	625	2.692	-1.6	5.75	+ 1	- 5	+14.0	+10	- 8	- 9	+261	- 29	-134
1443	327	2.652	-2.1	4.95	+ 7	- 2	+13.0	+ 3	-15	- 2	+ 64	-180	-180
1463*	196	2.612	-3.25	3.85	0	- 5	+14.9	+ 9	- 9	-10	+212	- 74	-137
1497*	580	2.700	-1.25	4.1	- 1	-17	+14.6	+13	- 6	-10	+113	+ 7	- 31
1552*	262	2.606	-3.6	3.4	- 2	0	+24.1	+21	- 3	-11	+225	- 51	-100
1553	536	2.691	-1.4	5.3	+ 1	- 4	+10.5	+ 9	- 5	- 5	+202	- 32	- 78
1582	621	2.694	-1.55	5.35	- 6	-13	+24.0	+10	-15	-23	+194	- 86	-112
1595	217	2.634	-2.45	6.1	- 6	- 6	+11.4	- 4	- 6	-22	+365	-242	-268
1600*	852	2.709	-1.25	5.6	+ 9	+ 4	+ 6.0	+ 9	- 3	+ 9	+222	- 24	- 68
1617	422	2.661	-2.0	4.7	0	+ 8	+25.4	+25	- 4	- 8	+173	- 87	-102
1640	357	2.665	-1.7	6.3	+ 4	- 2	+16.0	+10	-15	- 3	+284	-194	-200
1646	650	2.685	-1.85	5.9	- 8	0	+26.7	+20	- 2	-22	+296	-126	-150
1659*	365	2.637	-2.7	4.65	0	- 2	+15.9	+15	- 2	- 4	+291	+ 4	- 49
1713*	405	2.550	-5.7	0.1	- 1	- 3	+20.0	+14	-10	-10	+114	- 63	- 62
1731	396	2.657	-2.05	6.45	+ 6	- 3	+12.0	+ 5	-19	+ 4	+344	-275	-238
1735	789	2.687	-1.65	3.45	-18	- 9	+20.1	+13	- 7	-17	+ 85	- 45	- 43
1764	476	2.691	-1.2	5.5	- 7	+ 4	+ 7.2	+ 8	+ 5	- 7	+190	- 79	- 75
1790	249	2.614	-3.3	1.55	-11	-14	+18.2	+14	- 7	-12	+ 86	- 26	- 26
1810	323	2.642	-2.45	4.6	+ 4	-10	+11.8	+11	-14	- 4	+254	- 17	- 32
1840	402	2.646	-2.45	6.2	- 5	+ 1	+11.0	+10	+ 4	-14	+407	-239	-365

TABLE V - CONTINUED

HR	[u-b] ($0^m.001$)	β	M_V	V_O	μ_α ($0''.001$)	μ_δ ($0''.001$)	ρ (km/sec)	U (km/sec)	V (km/sec)	W (km/sec)	X (Parsecs)	Y (Parsecs)	Z (Parsecs)
1846	945	2.697	$-1^m.6$	$6^m.25$	- 2	- 2	+ 0.1	+ 1	- 1	- 5	+362	+ 80	+ 32
1864	493	2.685	-1.45	5.45	- 4	-10	+19.1	+15	-10	-13	+232	- 45	- 42
1951	588	2.697	-1.4	6.2	- 9	-13	+26.0	+24	-12	-24	+329	- 25	- 21
1962	570	2.666	-2.25	6.0	-12	- 4	+15.5	+ 4	- 1	-31	+312	-269	-173
2064	754	2.700	-1.4	5.1	-12	+14	+15.8	+12	- 9	-18	- 20	-170	-102
2075	834	2.703	-1.35	5.9	+ 3	- 8	+12.5	+ 8	-15	- 4	+266	- 87	- 38
2089	546	2.671	-2.05	5.95	- 3	+ 6	+12.2	+14	- 6	- 9	+ 79	-338	-195
2106	534	2.645	-2.8	4.3	0	+ 8	+24.2	+19	-15	- 8	+114	-208	-114
2205	336	2.634	-2.75	5.0	- 7	+ 2	+28.7	+26	- 8	-15	+287	-196	- 72
2229	1171	2.681	-1.95	5.4	0	- 1	+12.7	+12	- 5	- 1	+280	- 90	- 10
2271	540	2.656	-2.5	5.7	-11	+ 3	+30.9	+27	- 9	-26	+278	-314	-122
2325	536	2.674	-1.95	6.05	-13	- 3	+10.0	+ 9	0	-26	+326	-221	- 53
2344	383	2.652	-2.2	4.9	- 8	0	+24.5	+22	- 9	-13	+215	-148	- 34
2387	91	2.583	-4.3	4.15	- 3	+ 6	+26.7	+28	-11	- 7	+291	-375	-122
2461	924	2.718	-1.15	5.65	-14	- 4	+23.0	+21	- 9	-16	+196	-119	- 8
2475	580	2.678	-1.95	6.05	- 1	+ 4	+17.0	+13	-12	- 5	+133	-352	-129
2490	526	2.668	-1.9	5.05	+ 4	- 5	+ 5.3	+ 7	- 4	+ 6	+196	+123	+107
2497	713	2.716	-1.0	6.45	- 6	+ 2	+18.0	+13	-10	-11	+149	-259	- 78
2517	457	2.628	-3.2	5.85	- 6	- 5	+23.2	+17	-16	-23	+549	-340	0
2519	713	2.703	-1.35	5.75	-19	-11	+12.8	+15	- 7	-26	+248	- 81	+ 32
2571	108	2.594	-3.8	4.65	- 6	0	+30.7	+23	-18	-17	+302	-377	- 74
2619	533	2.693	-1.3	5.0	-19	+ 5	+19.2	+16	-10	-17	+ 76	-160	- 42
2648	127	2.596	-3.9	4.8	- 6	+ 1	+24.8	+25	- 7	-13	+453	-354	+ 6
2676	744	2.705	-1.3	6.0	-27	-16	+ 6.1	+ 8	- 8	-42	+248	-145	+ 29
2699	59	2.587	-4.15	5.1	-13	-10	+ 6.4	0	- 8	-54	+459	-537	- 42
2702	454	2.648	-2.55	4.75	-12	+ 9	+19.5	+22	-10	-14	+ 92	-264	- 69
2718	454	2.661	-2.1	5.8	-10	+ 4	+21.6	+23	- 9	-15	+198	-321	- 48
2726	521	2.699	-1.1	5.85	- 6	+ 2	+17.0	+11	-12	- 9	+ 89	-222	- 50
2739	- 17	2.602	-3.85	5.65	- 8	0	+32.6	+33	-13	-26	+565	-559	+ 5
2756	530	2.676	-1.85	5.3	-17	+15	+33.4	+33	-15	-16	+121	-236	- 41
2819	489	2.626	-3.1	5.25	-11	+ 2	+23.5	+22	-12	-23	+197	-420	- 64
2823	473	2.641	-2.8	5.35	- 9	+ 6	+21.3	+26	-10	-13	+178	-384	- 59
2845	1019	2.733	-1.05	2.85	-52	-39	+22.0	+20	-15	-13	+ 51	- 29	+ 12
2847	441	2.644	-2.65	6.2	- 4	- 5	+10.3	- 3	-10	-18	+247	-530	- 75
2856	456	2.651	-2.45	5.85	- 6	+ 7	+ 7.0	+20	+ 1	- 5	+175	-417	- 65
2928	187	2.620	-2.9	5.45	-11	+ 5	+22.0	+30	- 6	-16	+265	-386	+ 5
2961	490	2.662	-2.2	4.8	-20	+10	+26.0	+28	-16	-13	+ 77	-235	- 34
2963	705	2.715	-1.05	5.7	-22	+14	+30.0	+32	-18	-17	+ 72	-210	- 28
2964	553	2.647	-2.8	5.35	-13	+ 8	+22.6	+32	-11	-18	+130	-402	- 58
3004	216	2.600	-3.75	5.45	+ 1	+11	+15.0	+33	+ 1	+21	+338	-604	- 3
3016	451	2.678	-1.55	6.2	-15	- 6	+24.0	+10	-18	-30	+107	-336	- 42
3023	250	2.643	-2.2	5.75	- 2	+ 8	+ 7.0	+16	+ 1	+ 4	+199	-334	+ 9
3035	437	2.640	-2.75	4.75	-22	- 3	+12.2	+14	- 4	-32	+191	-300	- 36
3055	- 3	2.592	-4.3	3.8	- 4	+ 5	+24.0	+16	-19	- 6	+ 70	-404	- 74
3058	167	2.608	-3.35	5.55	- 2	+ 8	+25.2	+27	-21	+ 2	+ 96	-585	-107
3059	754	2.684	-1.8	5.0	-18	- 3	+32.3	+32	-17	-10	+174	-137	+ 56
3074	375	2.607	-3.75	6.2	-12	+ 1	+14.0	+32	0	-47	+210	-944	-140
3089	191	2.611	-3.25	4.45	- 3	+18	+ 8.0	+29	- 7	+ 8	+ 39	-337	- 67
3107	363	2.658	-1.95	6.7	-13	+ 2	+13.8	+23	- 5	-27	+130	-518	- 58
3116	467	2.648	-2.6	4.9	- 7	+ 3	+15.8	+12	-12	- 9	+ 60	-307	- 43

TABLE V - CONTINUED

HR	[u-b]	β	M_V	V_O	μ_α	μ_δ	ρ	U	V	W	X	Y	Z
	($0^m.001$)				($0''.001$)		(km/sec)		(km/sec)			(Parsecs)	
3117	499	2.654	$-2^m.45$	$3^m.45$	-29	+27	+19.4	+28	-16	-13	+ 9	-147	- 32
3137	530	2.672	-2.0	5.85	- 2	+ 3	- 2.7	+ 5	+ 4	0	+ 64	-362	- 53
3139	919	2.711	-1.3	6.05	-16	+ 8	+23.0	+18	-19	-21	- 30	-280	- 87
3156	639	2.692	-1.6	5.9	-18	+ 4	0.0	+19	+ 5	-20	+ 11	-309	- 68
3168	389	2.619	-3.35	6.0	-10	0	+13.8	+25	- 5	-28	+381	-630	+ 82
3192	589	2.684	-1.8	4.3	-17	- 9	+19.0	+12	-17	-12	+ 85	-141	-121
3204	389	2.616	-2.9	5.2	- 7	- 5	+ 8.0	0	- 6	-18	+ 71	-409	- 43
3213	163	2.603	-3.5	5.15	+ 6	+ 9	+ 5.0	+12	- 7	+24	+ 62	-528	- 75
3223*	735	2.711	-1.15	4.2	- 4	+27	+ 9.6	+12	-13	+ 2	- 22	-109	- 37
3227	510	2.678	-1.75	5.85	-15	+ 2	+14.6	+17	-10	-20	+ 35	-326	- 46
3240	226	2.614	-3.25	4.9	- 7	+ 8	+18.0	+25	-11	- 3	+118	-410	- 7
3244	547	2.657	-2.5	5.05	- 9	+ 5	+25.0	+19	-20	- 9	+ 71	-315	- 18
3250	323	2.636	-2.65	5.55	- 1	- 1	+20.0	+ 2	-19	- 5	+ 61	-430	- 47
3283	301	2.610	-3.55	5.1	- 2	+ 1	+16.0	+ 9	-14	- 3	+140	-518	+ 1
3330*	467	2.662	-2.15	5.0	-16	+21	+18.0	+34	-16	- 4	+ 34	-266	- 37
3343*	455	2.683	-1.4	6.45	- 8	+ 3	+23.6	+18	-20	- 7	+ 98	-358	+ 13
3356	415	2.597	-4.15	5.65	+ 1	+ 6	+ 3.0	+19	- 1	+19	+126	-902	- 49
3375	494	2.653	-2.5	6.35	-12	+ 5	+11.0	+32	- 7	-20	+ 48	-585	- 51
3440	559	2.693	-1.6	5.45	-25	+ 8	+15.0	+26	-13	-20	- 2	- 55	- 32
3442*	658	2.692	-1.65	5.0	-17	+19	+14.0	+26	-14	- 3	- 1	-212	- 26
3453	162	2.592	-3.95	5.8	- 1	+ 2	+18.0	+10	-17	+ 1	+ 45	-888	- 66
3457*	192	2.596	-3.85	3.95	- 2	+10	+12.9	+14	-16	+ 5	- 36	-355	- 68
3467*	508	2.674	-2.1	4.65	-19	+15	+19.0	+25	-18	- 8	- 2	-222	- 26
3468	170	2.606	-3.4	3.45	-15	+12	+15.3	+24	-10	- 3	+ 60	-226	+ 24
3560	571	2.650	-2.75	5.5	- 4	+13	+ 2.0	+26	- 7	+10	- 56	-436	- 77
3562	508	2.654	-2.5	6.2	+ 1	+ 6	+22.0	+12	-20	+12	+ 44	-548	- 2
3658	249	2.629	-2.75	5.75	0	+ 2	+ 7.0	+ 4	- 7	+ 3	+ 12	-501	+ 10
3663*	487	2.661	-3.2	3.9	-36	0	+17.8	+31	-17	-25	+ 53	-252	+ 50
3672	667	2.700	-1.35	5.75	-24	+12	+20:	+31	-19	-10	+ 12	-250	+ 14
3674	590	2.686	-1.7	5.15	-25	+16	+13.0	+33	-12	- 7	+ 14	-233	+ 15
3683	1056	2.738	-1.0	5.35	-22	+ 1	+ 9.7	+18	- 7	- 9	+ 84	-144	+ 84
3717	584	2.644	-2.95	5.8	-12	- 1	+12.5	+19	-13	-25	- 56	-558	- 38
3924	394	2.626	-3.1	5.8	- 6	+ 2	+ 7.6	+16	-10	- 6	- 72	-598	+ 27
3940	509	2.597	-4.3	3.2	- 9	+ 8	+14.0	+16	-17	+ 1	- 51	-312	+ 1
3949	521	2.678	-1.75	5.5	-12	- 1	+11.1	+ 8	-12	-13	- 87	-262	- 55
3952	417	2.654	-2.25	5.6	-13	+ 3	+ 3.0	+21	0	-10	+198	-120	+291
3975	1118	2.652	-2.45	3.3	+ 1	- 2	+ 2.9	0	- 2	+ 3	+ 39	- 47	+124
3982*	910	2.723	-1.05	1.3	-247	+ 7	+ 3.5	+29	- 6	-17	+ 13	- 14	+ 22
4038	357	2.637	-2.7	6.05	-15	- 1	+10.0	+29	-17	-24	-114	-551	+ 13
4074*	603	2.642	-3.05	4.35	-18	- 5	+10.5	+15	-14	-20	- 68	-294	+ 5
4329	394	2.662	-1.9	5.75	-26	- 5	+ 7.4	+23	-15	-19	-105	-230	- 43
4389	550	2.694	-1.35	6.15	-21	- 6	0.0	+25	- 8	-19	-136	-280	- 57
4390*	568	2.696	-1.35	4.15	-28	- 2	+13:	+12	-19	- 7	- 51	-139	+ 16
4415	538	2.637	-3.05	4.85	-12	+ 9	+ 9.4	+20	-19	+ 8	-147	-350	+ 1
4467	1350	2.743	-1.0	3.0	-38	- 4	+ 7.9	+ 7	-12	- 5	- 26	- 57	- 2
4472	490	2.637	-3.0	5.5	- 5	+ 7	+13.0	+10	-18	+13	-203	-458	+ 5
4603*	464	2.664	-2.05	4.4	-10	+14	+16.3	0	-18	+13	-110	-161	- 1
4743	327	2.656	-1.95	3.8	-27	-18	+23.0	+ 8	-20	-11	- 67	-120	+ 30
4773	553	2.695	-1.3	3.75	-48	- 5	+ 3.6	+18	-14	- 5	- 53	- 86	- 17
4798	280	2.645	-2.25	2.55	-40	-12	+11.8	+ 9	-18	- 7	- 48	- 77	- 10

TABLE V - CONTINUED

HR	[u-b]	β	M_V	V_O	μ_α	μ_δ	ρ	U	V	W	X	Y	Z
	(0.001)				(0.001)		(km/sec)		(km/sec)			(Parsecs)	
4944*	1090	2.709	-1.5	5.0	-21	-10	+ 4.0	+14	-15	- 8	-114	-164	+ 10
4967	730	2.711	-1.15	6.25	-17	+ 7	- 5.5	+25	- 7	- 6	+ 17	+ 61	+295
5056*	159	2.608	-3.3	0.9	-41	-29	+ 1.0	+ 6	-12	- 3	- 31	- 30	+ 54
5063	406	2.616	-3.5	6.0	- 1	+ 2	- 4.5	+ 7	+ 3	+ 6	-486	-602	+180
5132	144	2.610	-3.2	2.2	-22	-13	+ 5.6	+ 6	-14	- 4	- 77	- 91	+ 18
5221*	621	2.665	-2.4	4.6	- 7	- 9	+ 5.2	+ 1	-14	- 4	-163	-147	+122
5469	200	2.604	-3.55	2.1	-19	-16	+ 7.5	+ 3	-17	- 3	-103	- 82	+ 27
5500	377	2.635	-2.8	5.6	+ 1	-17	+19.0	0	-20	-38	-332	-341	- 53
5539	475	2.673	-1.8	5.6	+ 3	-14	-16.7	+17	+ 9	-18	-213	-212	- 32
5626*	466	2.686	-1.35	4.5	-11	-22	+10.2	- 2	-18	- 7	-121	- 79	+ 28
5661	17	2.605	-3.65	5.2	- 3	+ 2	+ 4.0	0	- 6	+ 9	-449	-380	- 29
5668	481	2.658	-2.3	5.85	- 6	-16	-21.0	+28	-15	-25	-357	-215	+ 88
5781*	450	2.685	-1.3	4.45	- 9	-22	+ 7.9	- 1	-16	- 7	-122	- 68	+ 21
5873*	164	2.593	-3.9	4.9	- 4	- 5	- 0.2	+10	-14	- 4	-482	-315	- 7
5904*	377	2.680	-1.25	4.2	-15	-25	-10.0	+11	-14	- 8	-111	- 26	+ 45
5953	56	2.602	-3.6	1.8	-10	-23	- 3.4	+ 3	-13	- 6	-109	- 19	+ 46
6083	747	2.707	-1.3	5.1	- 8	-33	-10.4	+21	-19	-16	-171	- 83	0
6084*	61	2.609	-3.3	1.7	-10	-21	- 0.1	0	-10	- 3	- 94	- 14	+ 29
6092	609	2.702	-1.3	3.8	-12	+39	-13.8	+23	- 6	- 7	- 22	+ 71	+ 74
6115*	540	2.693	-1.35	4.85	-15	-16	-12.5	+19	-11	- 1	-159	- 71	+ 3
6141	365	2.662	-1.85	4.5	- 3	-26	- 5:	+ 4	-18	-13	-170	- 20	+ 48
6143	261	2.647	-2.1	4.0	-10	-16	- 4.5	+ 7	-13	- 4	-159	- 40	+ 27
6215	405	2.634	-2.85	5.35	+ 4	- 5	-16.0	+17	+ 5	-11	-372	-217	- 65
6396	-	-	-1.9:	3.1	-21	+20	-14.1	+ 9	-17	- 2	+ 9	+ 81	+ 57
6414*	510	2.700	-1.0	5.85	- 2	-12	-11.5	+ 3	-15	- 8	-201	+ 84	+ 66
6431*	360	2.848	-2.3	4.65	- 2	- 5	-21.0	+ 5	-18	-11	-113	+171	+134
6447	816	2.688	-1.65	5.55	- 3	- 7	-10.0	+14	- 4	+ 1	-234	-131	- 65
6453*	266	2.617	-3.2	3.15	- 3	-21	+ 2.7	- 4	-17	- 8	-185	+ 1	+ 21
6462	29	2.560	-5.45	2.9	+ 4	-14	- 5.4	+18	-15	-23	-414	-197	- 93
6471	862	2.702	-1.45	6.1	+ 3	-14	- 3.0	+14	-10	-14	-268	-161	- 85
6502	611	2.688	-1.7	5.2	+ 7	+17	-29.5	+32	- 2	-14	-157	+145	+110
6527*	201	2.614	-3.15	1.45	+ 1	-29	- 7.0	+ 9	- 8	- 6	- 82	- 12	- 3
6580	203	2.614	-3.15	2.3	- 8	-28	-10:	+13	-14	- 4	-121	- 19	- 10
6588	449	2.661	-2.1	3.7	- 6	+ 4	-20.0	+ 8	-18	- 7	- 37	+117	+ 75
6619	1116	2.648	-2.5	6.1	+ 3	- 1	+ 2.4	- 3	+ 4	- 6	-259	+390	+238
6622*	465	2.668	-1.9	5.85	+ 9	- 8	- 6.0	+11	- 1	-18	-322	-124	- 81
6628	952	2.720	-1.15	4.6	+10	-16	-13.0	+14	- 5	-11	-142	- 5	- 5
6684	209	2.630	-2.6	4.7	- 7	+ 2	-17.6	+16	-11	+ 6	-250	+128	+ 62
6719	243	2.624	-2.9	5.8	- 1	- 3	-16.5	+ 9	-15	- 5	-448	+289	+134
6720	868	2.723	-1.0	6.2	+24	- 5	-29.0	+16	- 7	-39	-182	+185	+ 93
6738	458	2.685	-1.35	4.95	+ 3	- 9	-14.9	+ 4	-13	-10	-117	+125	+ 62
6787	279	2.608	-3.55	4.05	+ 3	- 6	-14.5	+ 3	-13	-12	-213	+231	+105
6851	570	2.687	-1.65	5.85	+ 1	0	-20.7	+15	-13	- 6	-252	+224	+ 81
6924*	540	2.692	-1.35	6.3	+ 5	+ 1	-21:	+14	-12	-13	-188	+264	+ 98
6938*	615	2.667	-2.35	4.9	-12	- 8	- 7.6	+ 7	-15	+12	-266	- 51	- 77
6941	441	2.655	-2.3	5.75	+ 2	- 7	-18.5	+ 8	-18	-12	-335	+227	+ 47
6946*	318	2.641	-2.45	4.3	+14	-16	-11.8	+ 8	-12	-21	-209	- 80	- 2
6971	639	2.681	-1.95	6.4	+ 8	- 5	- 4.0	- 4	0	-21	-227	+385	+138
7040	1056	2.718	-1.35	4.85	+ 4	-17	-15:	+ 6	-17	-10	-144	+ 97	+ 7
7081	454	2.657	-2.25	5.8	- 3	- 1	-15.0	+ 4	-16	+ 1	-188	+346	+102

TABLE V - CONTINUED

HR	[u-b]	β	M_V	V_O	μ_α	μ_δ	ρ	U	V	W	X	Y	Z
	($0^m.001$)				($0''.001$)		(km/sec)		(km/sec)			(Parsecs)	
7100	393	2.660	$-1^m.95$	$5^m.7$	+ 6	- 3	-16.5	+ 6	-12	-15	-151	+291	+ 86
7121	395	2.668	-1.7	2.05	+14	-55	-11.4	+11	-14	- 7	- 54	+ 9	- 12
7171	759	2.699	-1.45	6.15	- 1	- 5	- 1.0	- 6	- 5	- 2	-205	+257	+ 42
7173	332	2.616	-3.4	5.35	+ 7	- 1	-18:	+17	- 7	-19	-412	+382	+ 28
7179	487	2.667	-2.05	6.1	+ 6	+ 4	-19.0	+17	-11	-13	-134	+387	+118
7185	438	2.692	-1.0	6.25	0	+ 5	-14.0	+11	-11	- 1	- 95	+254	+ 75
7200*	203	2.640	-2.2	5.9	+ 3	- 2	-10.3	+ 5	- 8	- 8	-251	+329	+ 53
7202	596	2.687	-1.7	5.4	+ 7	- 6	-14:	+ 4	-12	-13	-139	+219	+ 44
7210	413	2.675	-1.5	5.3	+ 6	+11	-19.0	+16	-15	- 8	- 35	+213	+ 76
7212	526	2.594	-4.4	6.15	+ 2	- 2	-22.9	+ 3	-19	-21	-542	+1134	+282
7258*	506	2.690	-1.35	6.35	+ 5	- 1	-21.2	+ 7	-17	-13	-103	+319	+ 89
7262	651	2.652	-2.75	5.15	+ 2	- 2	-18:	+ 5	-16	- 9	-144	+342	+ 83
7269	601	2.679	-1.95	5.9	+ 5	- 5	-11.2	+ 8	-10	-11	-305	+211	- 28
7279	505	2.637	-3.0	4.35	+14	- 8	-15.4	+16	-10	-20	-257	+138	- 43
7287	794	2.718	-1.0	4.95	+ 8	0	- 5.2	+ 6	0	- 5	-122	+ 94	- 11
7298	484	2.634	-3.05	4.2	+ 2	0	- 8.2	+ 4	- 7	- 4	- 91	+259	+ 62
7372	375	2.667	-1.7	4.65	+18	+12	-21:	+24	-10	-11	- 84	+165	+ 21
7374	593	2.706	-1.1	6.2	- 5	+10	-19.5	+18	-14	+10	-137	+252	+ 29
7397	712	2.691	-1.65	5.3	+11	-10	-13.5	+ 9	-13	-15	-187	+156	- 29
7426	557	2.656	-2.55	4.55	+ 2	- 2	-21.8	+ 7	-19	- 6	- 98	+242	+ 34
7466	648	2.691	-1.65	6.2	+10	+ 2	-20.1	+25	- 9	-23	-257	+528	+ 41
7474*	325	2.647	-2.25	5.0	+ 5	- 5	- 4.8	+ 3	- 6	- 8	-203	+191	- 39
7516	426	2.649	-2.45	5.65	0	0	-17.4	+14	-10	+ 4	-325	+242	- 97
7651	500	2.668	-2.0	6.1	+ 6	+ 5	-16.2	+15	-14	- 8	- 28	+407	+ 83
7656	622	2.704	-1.3	5.7	+ 7	- 6	-15.0	+ 6	-14	-10	-115	+223	- 13
7688	483	2.686	-1.4	4.95	+18	- 1	- 5.4	- 1	- 2	-13	- 86	+165	- 15
7709	80	2.597	-3.75	6.1	+ 1	- 1	- 7.0	+ 6	- 6	- 3	-719	+484	-345
7739*	438	2.658	-2.15	4.65	+10	- 3	- 5.0	+ 6	- 4	-10	- 96	+207	- 21
7757	759	2.654	-2.45	6.3	+ 8	+ 2	- 6.0	+17	- 1	-15	-147	+543	+ 10
7789*	787	2.672	-2.0	5.2	+ 2	- 7	-13.0	+ 1	-15	- 6	-115	+248	- 34
7861*	565	2.672	-2.05	6.35	+ 4	+ 5	-16.9	+17	-15	- 1	- 69	+473	+ 16
7862	451	2.688	-1.2	6.25	+14	- 1	+ 3.1	+10	+ 4	-18	-134	+272	- 61
7912	530	2.679	-1.75	6.15	+ 5	+ 3	-15.7	+11	-14	- 4	- 37	+378	+ 17
7929	443	2.651	-2.4	5.05	+ 1	+ 5	- 3.3	+ 7	- 3	+ 3	- 9	+308	+ 27
8007*	92	2.614	-3.05	6.15	+ 8	- 7	- 8.0	+ 3	-14	-33	-202	+650	-126
8022	674	2.710	-1.15	6.4	+13	+ 4	-18.4	+18	-17	-12	+ 2	+322	+ 21
8029	461	2.682	-1.45	6.1	+ 6	+ 5	-19.0	+10	-19	- 5	+ 27	+320	+ 42
8107	761	2.693	-1.6	6.0	+ 1	+ 5	- 8.8	+ 7	- 9	+ 4	- 4	+331	- 2
8144	714	2.683	-1.85	6.05	+16	- 7	-20.3	+13	-19	-28	- 23	+378	- 30
8226	854	2.709	-1.25	5.25	+15	+11	- 7.0	+27	-10	- 4	+ 38	+363	+ 17
8238*	127	2.608	-3.3	2.9	+13	+ 9	- 6.7	+10	-10	- 4	+ 51	+161	+ 42
8292	733	2.711	-1.15	5.9	+15	- 5	+ 5.5	+ 8	- 1	-18	- 90	+202	-130
8301*	458	2.642	-2.75	4.35	+ 7	+ 3	- 8.2	+ 8	- 9	- 3	+ 25	+262	- 6
8335*	392	2.617	-3.45	3.85	+ 5	- 1	-12.3	+ 3	-13	- 5	+ 24	+287	- 16
8341	417	2.647	-2.45	5.9	+ 9	- 4	-15.1	+13	-19	-12	-107	+410	-199
8356*	511	2.675	-1.85	4.95	+11	- 1	-19.0	+12	-19	- 1	- 36	+210	- 85
8384	345	2.654	-2.05	5.9	+ 3	+ 3	+ 2.4	+ 8	0	+11	+109	+368	+ 61
8385	553	2.661	-2.35	5.8	+15	+ 8	- 5.4	+33	+ 2	- 6	-141	+312	-253
8439	404	2.627	-3.1	5.65	- 3	- 2	- 5.2	- 4	- 6	+ 8	-278	+210	-422
8513	632	2.633	-2.2	4.85	+17	+ 1	- 7.5	+20	- 9	- 6	- 69	+182	-168

TABLE V - CONTINUED

HR	[u-b] ($0^m.001$)	β	M_V	V_O	μ_α ($0''.001$)	μ_δ	ρ (km/sec)	U	V	W (km/sec)	X	Y	Z (Parsecs)
8523*	664	2.690	-1.7	4.5	+26	- 5	- 9.5	+14	-14	-14	+ 23	+170	- 27
8535	605	2.694	-1.55	6.0	+16	+ 1	-13.2	+17	-17	-12	+ 78	+314	0
8579	303	2.625	-3.0	4.05	- 3	- 7	- 8.0	- 6	- 8	- 3	+ 32	+250	- 56
8606*	542	2.678	-1.85	5.85	+ 3	+ 1	-15.3	+ 2	-16	+ 1	+ 70	+337	- 43
8706	739	2.706	-1.3	6.15	0	-10	+ 6.5	- 4	+ 3	-14	+ 49	+291	- 92
8723	809	2.714	-1.1	5.45	+22	+ 5	+ 0.9	+21	- 4	- 5	+ 28	+189	- 73
8725	208	2.639	-2.25	5.3	+ 2	- 2	-13.0	- 1	-14	0	+ 59	+305	- 91
8733	290	2.693	-1.6	5.75	+ 1	- 3	-15.5	- 3	-16	+ 1	+ 49	+276	- 94
8745	934	2.707	-1.4	6.05	+ 3	+ 3	-10.8	+ 2	-12	+ 2	+102	+292	0
8762	561	2.661	-2.4	3.35	+23	- 5	-14.0	+ 9	-18	- 5	+ 29	+132	- 39
8770	562	2.691	-1.5	6.2	+ 8	+12	-12.6	+16	-17	+14	+106	+329	- 31
8797	16	2.598	-3.95	4.2	+ 7	0	- 8.5	+ 9	-12	- 5	+145	+401	- 6
8803*	296	2.664	-1.6	5.8	+ 6	+ 4	- 4.6	+ 8	- 8	+ 3	+104	+284	- 3
8858	613	2.677	-2.0	4.3	+20	- 8	- 6.0	+13	-14	- 3	- 38	+ 92	-184
8873	827	2.718	-1.05	6.1	+18	- 4	- 6.5	+16	-15	-10	+ 52	+240	-111
8926*	472	2.681	-1.55	5.5	+19	+ 6	-15.0	+ 9	-20	0	+ 69	+168	- 8
8965	978	2.728	-1.05	4.3	+30	0	- 0.5	+14	- 7	- 5	+ 37	+106	- 36
9005	202	2.634	-2.45	5.3	+ 4	- 3	-14.0	0	-14	- 8	+158	+316	+ 29
9071	168	2.608	-3.3	4.3	+ 8	- 1	-12.6	+ 5	-17	- 3	+142	+297	- 37
9087*	697	2.703	-1.35	4.95	+12	-10	+23:	+ 6	- 1	-26	+ 7	+ 82	-162
9091*	690	2.700	-1.45	4.95	+21	+ 7	+ 9.3	+17	- 2	-14	- 34	+ 10	-180

Notes to Table V

154 Sp.B. 143 days; 2 spectra.

208 Sp.B. 33.8 days.

779 β CMa variable.

836 Sp.B. 3.8 days.

1239 λ Tau, eclipsing binary 4.0 days. Grant's (1959) analysis gives A4 IV and $M_V = +0^m.6$ for the secondary with masses of 6.1 and 1.6 and radii of 6.0 and 4.0 for the primary and secondary, respectively, in solar units. The primary is then almost identical with HR 1044 (Eggen 1974b, Table 5) at the top of the evolved main sequence of the α Persei cluster.

1378 ADS 3179B, 29" distant, is an AO V star with $(V,B-V,U-B)_0 = (6^m.8,-0^m.01,-0^m.03)$ and $M_V = -0^m.1$ from the adopted modulus.

1463 β CMa variable.

1497 Sp.B. 3.5 days. Possibly a secondary spectrum.

1552 Sp.B. 5 days.

1600 ADS 3579B, 40" distant, is of type B6 IV with $(V,B-V,U-B)_0 = (7^m.0,-0^m.12,-0^m.43)$ and $M_V = +0^m.15$ from the adopted modulus. Probably an optical pair.

1659 Sp.B. 58.3 days.

1713 Rigel, Sp.B. 9.9 days.

Notes to Table V - Continued

3223 Sp.B. 14.2 days. Possibly a secondary spectrum.

3330 Proper motion has a p.e. of $0\overset{''}{.}006$.

3343 Very close binary, V_0 corrected for equal components.

3442 Sp.B. 3.1 days.

3457 Sp.B.

3467 Cpm with HR 3466 an Ap star with $(V,B-V,U-B)_0 = (5\overset{m}{.}4,-0\overset{m}{.}20,-0\overset{m}{.}58)$; the companion is itself double.

3663 Proper motion has a p.e. of $0\overset{''}{.}007$.

3982 Cpm companion, KO V, with $(V,B-V,U-B)_0 = (8\overset{m}{.}1,+0\overset{m}{.}85,+0\overset{m}{.}50)$.

4074 Proper motion has a p.e. of $0\overset{''}{.}006$.

4390 Visual binary with nearly equal components and a period of 39 years. The orbital elements give a mean mass of 14 times the sun but this is very uncertain.

4603 Sp.B. 3.4 days.

4944 V_0 corrected for equal components.

5056 Spica, Sp.B. 4 days; β CMa variable.

5221 Sp.B. 6.9 days.

5626 The value of V_0 is corrected for nearly equal components. The period is 72.9 years and the orbital elements give a mean mass of about 20 times the sun with the modulus adopted here.

5781 The proper motion has a p.e. of $0\overset{''}{.}007$.

5873 The proper motion has a p.e. of $0\overset{''}{.}006$.

5904 A $6\overset{m}{.}6$ companion, 3" distant, is included in the photometry.

6084 Sp.B. 34.1 days; β CMa variable.

6115 Sp.B. 3.3 days with equal components. Cpm companion 24" distant, B9 V, has $(V,B-V,U-B)_0 = (6\overset{m}{.}7,-0\overset{m}{.}12,-0\overset{m}{.}27)$ or $M_V = +0\overset{m}{.}5$.

6414 Eclipsing binary U Oph, equal components with a period of 1.7 days. The mean mass and radius are about 5 and 3 times the sun, respectively.

6431 Eclipsing binary 68 Her with a period of 2 days. The secondary spectrum may be present with a visual magnitude difference near one magnitude.

6453 β CMa variable ?

6527 Sp.B. 5.6 days ?

6622 Sp.B. 3.2 days, equal components.

6924 Cpm and radial velocity with HD 170051.

6938 Sp.B. 21.7 days.

6946 Herbig (1973) suggests shares its birth place with FK Ser.

7200 Sp.B. 16.0 days.

7258 Sp.B. 1.0 days.

Notes to Table V - continued

7474 σ Aql ellipsoidal variable ?, 2.0 days. V_O corrected for nearly equal components.

7739 Sp.B. 11.0 days.

7789 Possibly a weak helium star (See Table XI).

7861 Sp.B 5.4 days.

8007 BW Vul, β CMa variable.

8238 β Cep, β CMa variable. Cpm companion, 14" distant, A2 V with (V,B-V, U-B)$_0$ = ($7^m.5$,$+0^m.07$,$0^m.00$) and M_V = $1^m.3$ from the modulus adopted here.

8301 Sp.B. 26.3 days.

8335 Sp.B. 72.0 days.

8356 Sp.B. 17.8 days.

8523 Sp.B. 2.6 days, secondary about one magnitude fainter. Proper motion has p.e. of 0".006.

8725 Sp.B. 12.3 days; β CMa variable.

8803 Sp.B. 7.2 days, faint secondary spectrum.

8926 AR Cas, eclipsing binary 6.1 days.

8606 Sp.B. 10.9 days, faint secondary spectrum.

9087 Possibly a weak helium star (Table XI). (See Klinglesmith 1972.)

9091 The presently adopted modulus places the star 50 parsecs in front of the sparse cluster (ζ Scl cluster) at 240 parsecs but it seems reasonable to assume that this star, within 10° of the South Galactic Pole, is $0^m.5$ brighter and a member of the cluster Eggen (1970b).

TABLE VI

POSSIBLE MEMBERS OF THE OUTER ARM

HR	[u-b]	β	M_V	V_O	μ_α	μ_δ	ρ	U	V	W	X	Y	Z
	($0^m.001$)				(0".001)		(km/sec)		(km/sec)			(Parsecs)	
1072	180	$2^m.610$	$-3^m.25$	$5^m.6$	+ 1	- 8	+ 3.2	+ 8	-13	-17	+506	+285	- 94
1417B	- 23	2.605	-3.85	5.55	- 2	- 3	- 1.0	+ 1	- 3	-13	+669	+357	+ 52
1798	417	2.643	-2.6	5.85	- 5	-12	+31.5	+24	-20	-30	+477	- 67	- 87
2052	351	2.639	-2.6	5.8	- 5	- 9	+ 7.2	+ 4	-13	-20	+472	- 74	- 24
2276	579	2.647	-2.85	6.3	- 5	+ 1	+18.8	+21	+ 3	-13	+639	-220	- 16
8800	317	2.639	-2.55	6.1	- 2	+ 6	-16.1	- 2	-12	+19	+133	+506	-121
7567	195	2.580	-4.45	5.05	0	- 3	- 3.0	- 9	- 5	- 6	-201	+761	+ 98
7767	6	2.576	-4.9	4.6	0	- 3	- 7.0	- 8	- 8	- 7	-169	+774	+ 46
7977	19	2.530	-6.65	2.85	+ 2	- 4	- 8.0	- 6	- 8	-16	- 59	+792	+ 21
8248	See Text		(-5.0)	4.5	+ 1	- 2	- 5.2	- 3	- 6	- 8	+ 11	+792	- 60

identical clusters NGC 2323, NGC 2325, and NGC 2353, all at a distance of one kiloparsec near $(X, Y, Z) = (-750, -675, -30)$, show very little reddening. As noted elsewhere (Eggen 1974*b*), if these clusters constitute CMa OB 1 it is one of the oldest associations, because the clusters are about as old as the Hyades. Racine (1968) discussed the remarkable collection of reflection nebulae connected with this association.

An interesting comparison can be made between Figures 2 and 4 in the region of the largest concentration of group stars with $X = 0$ to -250 parsecs and $Y = 0$ to -250 parsecs. These stars are Southern Hemisphere objects and to avoid distortions due to the obvious tilt of Gould's Belt, with respect to the galactic plane, only stars between $\alpha = 12^h$ and 16^h will be considered in the comparison. The group stars in this part of the sky are shown as filled circles in the (X, Z) plane of Figure 5 and nongroup stars are indicated by open circles. Although the nongroup stars are few in number and are somewhat more dispersed, they could not be separated from group members on the basis of the strong (X, Z) correlation of the latter. However, in the (U, V) plane of Figure 6 the nongroup objects are clearly separated from the group members and indeed, within the uncertainties involved, could be characterized kinematically by $V = -16$ km sec^{-1} with a range of U that is the same as that for the group members. Whether or not the nongroup stars are regarded as belonging to Gould's Belt will obviously depend upon how membership in the belt is assigned. Stothers and Frogel (1974) give an extensive discussion of the history of Gould's Belt and adopt a positional criterion for member stars. The view that is adopted here is that the Pleiades group stars are relatively easy to isolate from kinematic considerations and this group, also called the local association, is identified with Gould's Belt because it contains most of the bright stars that, historically, have been associated with that belt. However, there may be other associations within this belt and the stars in Table VI may be part of such an association. The difficulty in applying positional criteria for separating Gould Belt stars from other interarm objects is further demonstrated in Figure 7. The (X, Z) distribution of the Pleiades group members and of the stars in Table V are shown in panels (a) and (b), respectively, whereas the (Y, Z) distributions are in panels (c) and (d), respectively. The well-known tilt of the Gould Belt distribution, with those nearer the galactic center lying mainly above the galactic plane, is well illustrated in Figure 7 (a) but even with the Pleiades group stars removed, that tilt is still apparent in Figure 7 (b). In general the distribution of both the group stars and the other interarm stars tangent to the direction of galactic rotation, Figures 7 (c) and (d), respectively, is

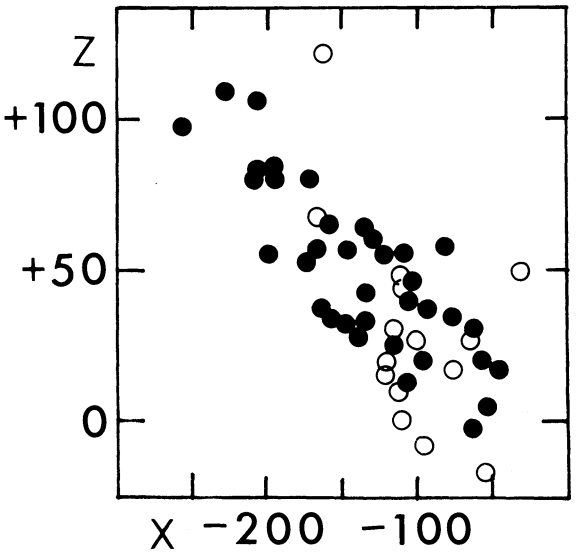

FIG. 5 — Pleiades group members (filled circles) and other interarm stars (open circles) in the region of Figures 2 and 4 bounded by $X = 0$ to -250 parsecs and $Y = 0$ to -250 parsecs.

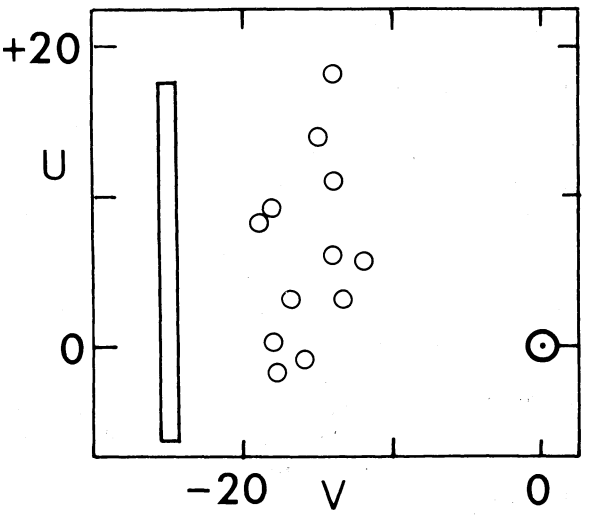

FIG. 6 — The nongroup stars of Figure 5 in the (U,V) plane. The group stars are in the rectangular region.

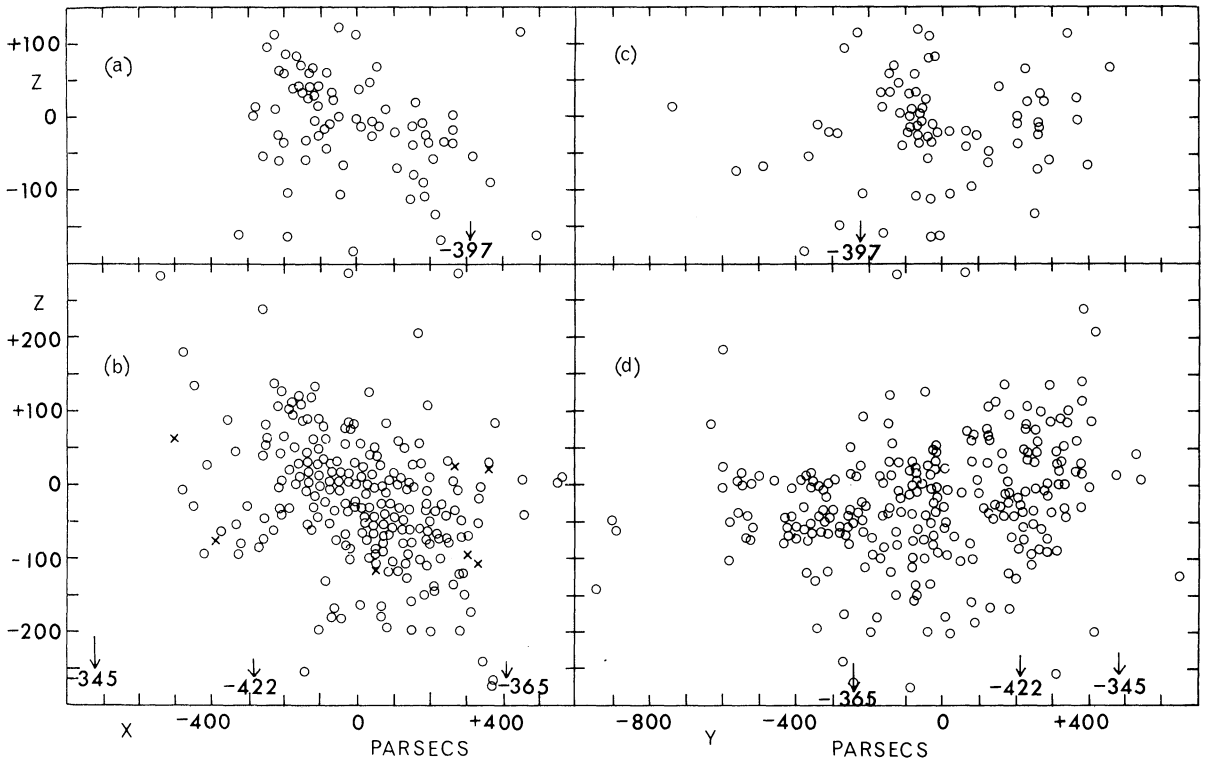

FIG. 7 — Group members (a and c) and nongroup stars (b and d) in the (X,Z) and (Y,Z) planes.

more random although there is a suggestion in Figure 7(d) that the stars preceding the sun (+Y) are more numerous above the galactic plane. The explanation of this latter effect, which may also be true for the distributions in Figures 7(a) and (b), is perhaps partly concerned with the distribution of absorbing clouds.

All of the stars in Table V are shown in the (U, V) plane of Figure 8. Obviously, if the stars in Figure 6 are part of a larger association, dispersed like the local association throughout Gould's Belt, that group will be difficult to identify from the kinematics alone.

Another region of overlapping concentrations of group and nongroup stars is in the direction of Orion at $X = +180$ to $+300$ parsecs and $Y = 0$ to -80 parsecs. Here the situation is reversed from that shown in Figure 5 in that there are fewer group stars but with one exception (HR 1520) they lie between the galactic plane and about 30 parsecs below the plane, as shown by the filled circles in Figure 9. On the other hand the nongroup stars, represented by open circles, are spread from 30 parsecs above the plane to 200 parsecs below. These nongroup stars, shown as open circles in Figure 10, have a larger dispersion in the (U, V) plane than those in the southern region discussed above, but again there is a clear separation from the Pleiades group stars. The position of the association Ori OB1 (Table I), which is also 100 parsecs below the galactic plane but at twice the distance of the stars discussed here, is shown as a filled circle in Figure 10. Kinematically, several of the objects in Figure 9 are indistinguishable from members of that association.

The stars of Table V are shown in the (M_V, $[u-b]$) plane of Figure 11 where schematic evolved main sequences, and the ZAMS are reproduced from Figure 3. These stars clearly show a wider distribution of ages than the group members in Figure 3.

There are several possible concentrations of kinematically related stars in Figure 4 but the one perhaps most deserving of attention contains eleven stars between 200 and 250 parsecs distant, in the anticenter direction. These objects, which are listed in Table VII, account for a large percentage of those in Figure 8 with values of U larger than +25 km sec^{-1}. A puzzling feature of

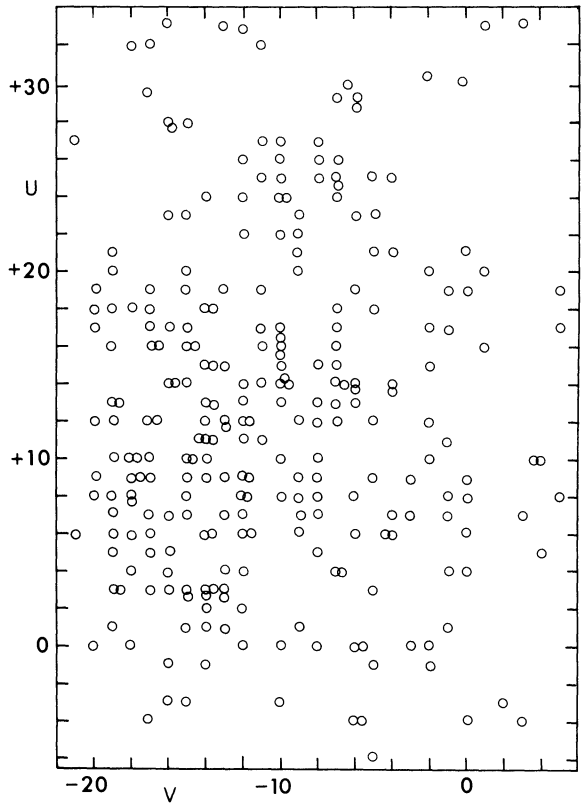

FIG. 8 — Nongroup stars in the (U,V) plane.

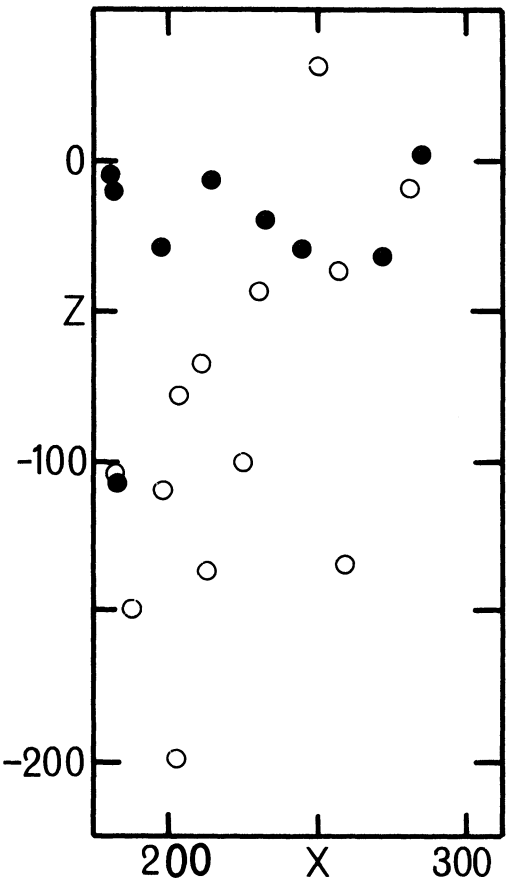

FIG. 9 — Same as Figure 5 but for the region bounded by $X = +180$ to $+300$ parsecs and $Y = 0$ to -80 parsecs in Figures 2 and 4.

this group of stars is that it contains three objects usually assigned to the cluster IC 2391 (HR 3440, HR 3442, and HR 3467). This cluster itself presents something of an enigma, with estimates of the modulus ranging from $5^m.9$ (Perry and Hill 1969) to $6^m.75$ (Graham 1967). A discrepancy was previously noted (Eggen 1972) between the modulus of $5^m.9$ obtained from the bright stars and $7:^m$ from the faint stars, both based on the Strömgren indices from observations by Perry and Hill. For the bright stars these indices show a systematic deviation from those published by Crawford and his associates (e.g., Eggen 1972, 1974*b*) and the same kind of discrepancy exists between the β values published by Perry and Hill (1969) and by Graham (1967). The present discussion is based entirely on the results by Crawford (Crawford and Barnes 1970; Crawford, Barnes, and Golson 1970, 1971; Crawford et al. 1973). Independent determination of the modulus by Buscombe (1965), based on spectra, and by Andrews (1968), based on photoelectric measurements of Hα, give $6^m.6$ and $6^m.9$, respectively. The cluster, which is spread over about 3°, is further marked by the absence of stars fainter than M_V near $+2^m.5$ (Lyngå 1968). It seems possible that rather than forming an isolated cluster, these stars are part of a more extended association. This association may also contain NGC 2451 (Eggen 1974*a*) to which two of the stars in Table VII may belong (HR 2961, HR 2963). The space motion of this cluster, which has a modulus of $6^m.55$, is $(U,V,W) = (+24, -17, -16)$ km sec^{-1}. Some fainter members of this cluster (Eggen 1974*a*, Table VIII) are shown in the $(M_V, [u-b])$ plane of Figure 12 as filled circles and the stars in Table VII are represented by open circles. The cluster Cr 140 is in the same direction but more distant (550 parsecs) and is apparently of the same age, as seen by the crosses in Figure 12, which represent the brightest stars (Eggen 1974*a*, Table VII).

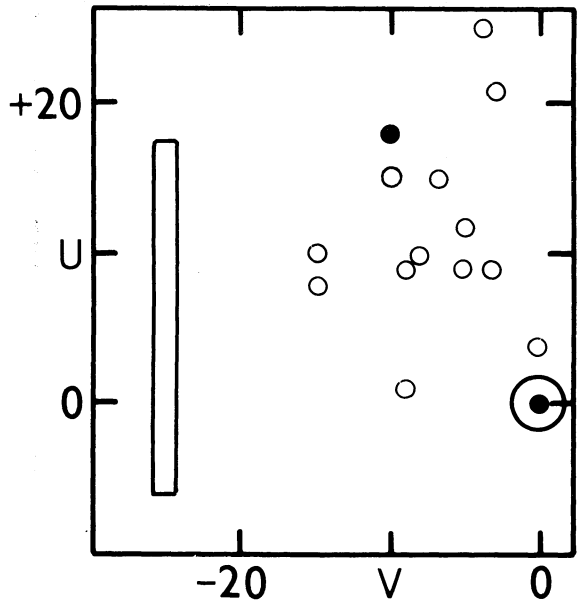

FIG. 10 — Nongroup stars (open circles) of Figure 9 in the (U,V) plane. The Ori 1 OB association (Table I) is shown by the filled circle and the Pleiades group stars are in the enclosed area.

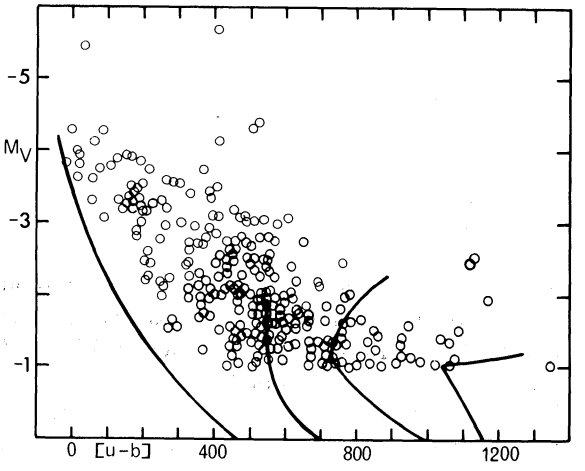

FIG. 11 — Nongroup stars (Table V) in the $(M_V,[u-b])$ plane.

These three clusters are of an age intermediate between the α Per cluster and the Pleiades.

The 34 stars listed in Table VIII show velocity vectors that are characteristic of old-disk-population objects. Three possibilities for the origin of these velocities are (1) incorrect proper motion or radial velocity, (2) the stars are blue stragglers of the old-disk population, or (3) they are runaway stars. The proper motions and radial velocities used here preclude the first possibility

TABLE VII

A POSSIBLE ASSOCIATION IN THE ANTICENTER DIRECTION NEAR 250 PARSECS

HR	U	V	W	X	Y	Z	V_O-M_V
	(km/sec)			(Parsecs)			
2702	+22	-10	-14	+ 92	-264	-69	$7^m.3$
2756	+33	-15	-16	+121	-236	-41	7.15
2961	+28	-16	-13	+ 77	-235	-34	7.0
2963	+32	-18	-17	+ 72	-210	-28	6.75
3330	+34	-16	- 4	+ 34	-266	-37	7.15
3440	+26	-13	-20	- 2	-255	-32	7.05
3442	+26	-14	- 3	- 1	-212	-26	6.65
3467*	+25	-18	- 8	- 2	-222	-26	6.75
3663	+31	-17	-25	+ 53	-253	+50	7.1
3672	+31	-19	-10	+ 12	-250	+14	7.1
3674	+33	-12	- 7	+ 14	-233	+15	6.85
	+29	-15	-12				6.95

*Cpm with HR 3466, an Ap (Si) star.

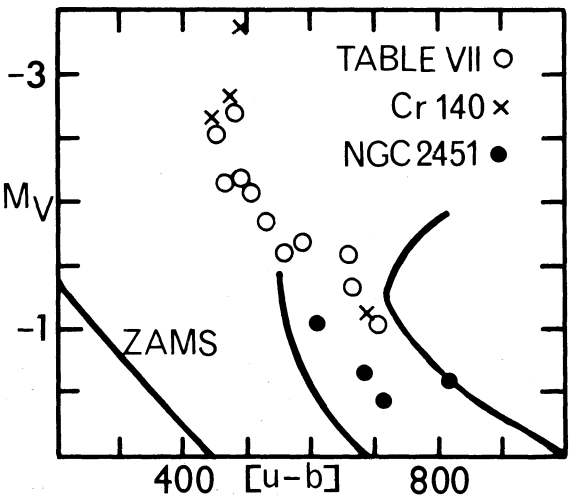

FIG. 12 — The possible group members (Table VII) compared in the $(M_V,[u-b])$ plane with stars in NGC 2451 and Cr 140. The schematic ZAMS and the evolved sequences for the Persei and Pleiades clusters are from Figure 3.

for all but one or two stars (e.g., HR 3388, HR 8141). A considerable number of these stars may be old-disk objects that are late evolvers because of some modification in the normal evolutionary process. From the position of the stars of Table VIII in the $(M_V,[u-b])$ plane of Figure 13, the most obvious candidates for old-disk-population stars are those with $[u-b]$ greater than about 600 and $M_V = -1^m$ to -2^m.

TABLE VIII

OLD DISK POPULATION OR RUNAWAY STARS

HR	[u-b]	β	M_V	V_O	μ_α	μ_δ	ρ	U	V	W	X	Y	Z
	($0^m.001$)				($0''.001$)		(km/sec)		(km/sec)		(Parsecs)		
189	609	2.702	$-1^m.3$	$5^m.4$	- 45	+ 10	-60.0	- 68	- 22	+27	+111	+180	- 57
938	239	2.657	-1.65	5.75	- 21	+ 7	+23.8	+ 5	+ 33	-22	+239	+ 73	-170
1174	534	2.684	-1.6	4.9	+ 28	- 27	+16.3	+ 17	- 36	- 7	+168	+ 8	-108
1194*	665	2.706	-0.9	5.95	+ 26	- 26	+16.3	+ 17	- 39	- 7	+196	+ 13	-117
1996*	- 11	2.598	-4.0	5.15	+ 6	- 22	+107.0	- 10	-118	-50	+325	-506	-308
2149	401	2.656	-2.1	5.6	- 15	+114	+92.8	+210	+ 12	- 3	+167	-271	-137
2177*	954	2.672	-2.05	4.9	0	- 5	+45.3	+ 12	- 39	-20	+ 98	-200	-100
2222	150	2.620	-2.85	5.9	+ 21	- 2	+36.0	+ 27	- 41	+46	+539	-160	- 15
2595	295	2.589	-4.3	5.15	0	- 8	+38.0	0	- 44	-19	+450	-619	-125
2633*	371	2.614	-3.5	5.9	- 9	- 18	+33.8	+ 13	- 56	-55	+656	-366	+ 64
2774*	573	2.676	-1.95	6.4	+ 19	- 4	+15.0	- 14	- 30	+31	+234	-401	+ 53
2799	534	2.667	-2.15	6.55	- 23	+ 2	+10.0	+ 31	+ 13	-51	+302	+458	- 40
3194	347	2.630	-2.95	8.5	- 15	- 16	+32.9	+ 11	- 41	-44	+272	-412	+ 79
3201	822	2.715	-1.1	5.9	- 8	- 20	+30.0	+ 20	- 34	- 6	+194	-126	+ 94
3388	478	2.653	-2.25	6.45	- 13	+ 9	+ 5.6	+ 38	+ 2	-12	+110	-513	+ 9
4133*	24	2.555	-5.6	3.55	- 7	- 2	+42.0	+ 31	- 31	+17	+238	-337	+542
4205	550	2.661	-2.35	4.65	- 21	+ 18	+25.5	+ 22	- 35	+ 5	- 84	-236	- 20
4221	947	2.664	-2.25	5.1	- 10	- 5	+31.0	0	- 33	-11	- 84	-283	+ 11
4234	440	2.682	-1.35	4.35	- 44	+ 12	+22.3	+ 17	- 30	-14	- 61	-116	- 45
4590*	234	2.607	-3.5	5.15	- 18	+ 5	+ 1.7	+ 45	- 15	+ 1	-117	-384	-357
4648	575	2.641	-3.05	5.6	- 35	- 12	-47.0	+ 86	- 12	-59	-207	-447	+213
4662*	966	2.719	-1.2	2.5	-162	+ 22	- 4.2	+ 46	- 17	- 5	- 16	- 42	+ 45
4674*	645	2.714	-1.0	4.05	- 43	+ 19	+23.0	+ 6	- 32	0	- 51	- 64	- 29
5039	758	2.640	-2.8	6.1	- 6	- 2	-41.0	+ 38	+ 20	-13	-362	-459	+146
5931	796	2.704	-1.3	6.15	- 7	- 16	-41.0	+ 11	- 37	-29	-180	-111	+226
6175*	- 23	2.578	-4.95	1.65	+ 12	+ 24	-20.0	+ 23	+ 27	- 4	-195	+ 21	+ 86
6353	88	2.626	-2.55	4.4	+ 7	+ 3	+16:	- 13	+ 14	+ 4	-213	+ 75	+ 96
6916	846	2.717	-1.1	4.55	+ 4	- 44	+59.2	- 30	- 46	-32	-112	- 57	- 50
7335	142	2.610	-3.25	6.35	- 13	- 26	+10:	-107	- 37	- 2	-336	+749	+135
7600*	76	2.597	-3.75	5.85	- 6	- 2	-65.0	- 9	- 69	+ 5	-117	+810	+149
7983	470	2.624	-3.35	5.9	+ 3	+ 21	-15.0	+ 61	- 12	+36	- 46	+699	+ 21
8141	667	2.703	-1.35	5.65	+ 14	+ 16	- 9.0	+ 25	+ 9	+ 1	-141	+152	-142
8438	675	2.643	-2.95	5.6	- 45	- 60	-51:	-164	- 95	-11	- 81	+449	-234
8682	645	2.671	-2.25	5.8	- 22	+ 2	-19.4	- 40	- 7	+24	+109	+391	- 31

Notes to Table VIII

1194 The colors, $(B-V,U-B)_0 = (-0.17,-0.56)$ and the spectral type B9 II-III (Osawa 1959) indicate a possible H-weak star. Cowley *et al.* (1969) call it Bp. The computed luminosity has therefore been reduced by $0^m.4$ (Eggen 1974a) and this puts it outside the limits defined. However it is retained in the table because of its possible connection with HR 1174, discussed in the text.

1996 μ Col.

2177 θ Col.

2633 p.e. of the proper motion is $0''.005$.

2774 p.e. of the proper motion is $0''.006$.

4133 ρ Leo.

NOTES TO TABLE VIII (Continued)

4590 Sp.B. 2.0 days.

4662 γ Crv. Probably a blue straggler in the Hyades Group.

4674 β Cha.

6175 ζ Oph.

7600 V 819 Cyg. Small amplitude variable of uncertain type.

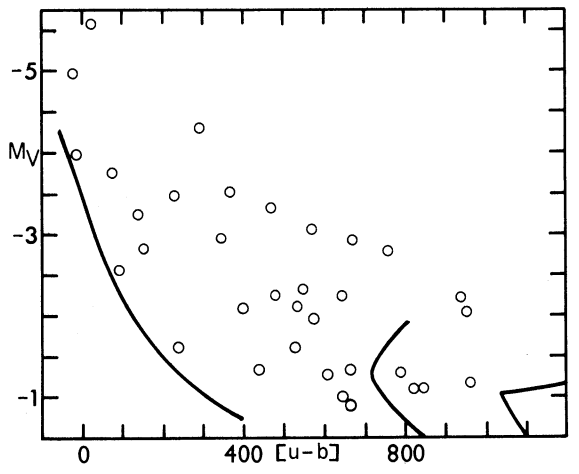

FIG. 13 — The aberrant velocity objects (Table VIII) in the (M_V,[$u-b$]) plane.

The runaway hypothesis (Blaauw 1961) is an attractive one to explain the motions of the hotter and brighter stars in Table VIII. Of the runaway stars suggested by Blaauw only 12 are bright enough to be in the present sample and four of these (HR 189, HR 1996, HR 2149, and HR 6175) are listed in Table VIII; one of the remaining stars shows Balmer emission making the Strömgren indices unreliable and the other seven are O-type stars with $[u-b] < -50$.

Attractive as it is, the suggestion that most of the stars in Table VIII are runaway relicts from a supernova explosion of a now-defunct companion star may be too easy a way to dismiss these aberrant motions. It may be accidental, but in this case the motion impressed by the supernova launching seems to have generally mimicked that of normal old-disk stars, with only a half-dozen objects receiving large, positive V velocities (HR 938, HR 5039, HR 6175) or excessive W velocities (HR 1996, HR 2799, HR 4648); and the ages of these objects are not great enough for such abnormal velocities to carry them beyond the horizon surveyed here. HR 1996 (μ Columbae) has nearly identical motion with Arcturus (U,V,W) = (−25, −116, −3) km sec^{-1} or HR 8834 (ϕ Aquarii) (−39, −116, −58) km sec^{-1}, and both of these latter objects are associated with a population (e.g., Eggen 1974*d*) that contains clusters with suprahorizontal branch stars that are only slightly fainter and cooler than HR 1996 (Zinn, Newell, and Gibson 1972). Also, it is difficult to reconstruct the explosive event that placed HR 1174 and HR 1194 so close together with the same velocity, although if they are runaways from the same event the fact that one may be a peculiar A-type star is of some theoretical importance. The motion of these two stars is similar to that of about a dozen other objects in Table VIII, as seen by the concentration in the (U, V) plane of Figure 14. Two of the stars in Table VIII are possible blue stragglers in the Hyades group (HR 4590 and HR 4662 (γ Corvi)) and the latter is only slightly brighter and hotter than a few other objects that are probable group members (Eggen 1970*a*).

VI. Age of Group Stars

The cluster NGC 2287 (Fig. 3) appears to mark the upper limit of the age of the Pleiades group stars (see Eggen 1974*b*, Fig. 7), which is near 8×10^7 years. There is also some evidence that the youngest group stars are still in the pre-main-sequence stage of their evolution.

One of the brightest of the T Tauri stars (Herbig 1962; Herbig and Rao 1972) is SU Aurigae, for which a reliable radial velocity, ρ = 23 km sec^{-1}, and proper motion from meridian observations, (μ_α, μ_δ) = (0.″000, −0.″035), are available. The visual light range is near one magnitude and at maximum light (V, $B-V$, $U-B$, $R-I)_0$ = $8^m.59$, $+0^m.74$, $+0^m.29$, $8^m.30$, $+0^m.31$) (Mendoza 1968); a reddening of $E(B-V) = +0^m.15$ has been adopted by Mendoza. The spectral type is

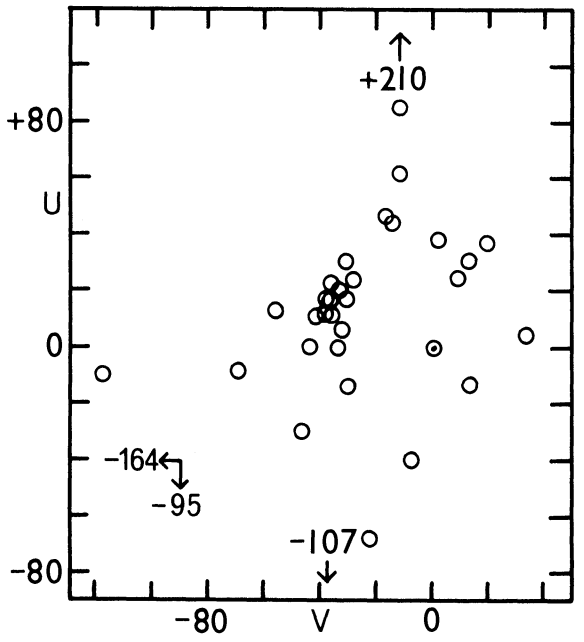

FIG. 14 — The stars of Table VIII in the (U,V) plane.

G2n III (Herbig and Rao 1972) and a distance of 215 parsecs gives (Eggen 1971*a*, Table 5) $M_{Bol} = M(I)_J + 1^m = +1^m9$ and $(U, V, W) = (+25, -25, -25)$ km sec^{-1}. Mendoza derives $M_{Bol} = +2^m5$ from an integration of the spectral energy distribution between 0.3μ and 2μ. In view of the nature of both determinations, the agreement is satisfactory. The variable is then in the Taurus dark cloud, slightly more distant than the α Per cluster ($R = 180$ parsecs and $U, V, W = +14, -25, -6$). Herbig (1962) points out that the four T Tauri stars, including SU Aur, in the Taurus dark cloud that have the most suitable spectra and the most material available for measurement all have radial velocities within 1 or 2 km sec^{-1} of that for SU Aur. Another of these four stars, RY Tau, has a similar, but less-accurately determined proper motion, based on photographic positions, $(\mu_\alpha, \mu_\delta) = (+0''.007, -0''.028)$, and is also a probable group member.

The star AB Aur forms a wide (3′) common proper-motion pair with SU Aur. Two additional, faint T Tauri stars near this pair, GM Aur and UY Aur, with radial velocities of +24 and 30 km sec^{-1}, respectively, may also share the motion but the proper motions are not available. AB Aur is one of the small group of Be- and Ae-type stars described by Herbig (1960), who believed it possible that they represent still contracting stars of relatively large mass but could find no convincing proof that this possibility is correct. However, the presence of AB Aur and SU Aur in a single system, and, especially, the common proper-motion system of HR 5999 and HR 6000, described below, may provide this proof. Although AB Aur is catalogued as a variable with over one magnitude visual range, there is no convincing evidence that the range exceeds a few tenths of a magnitude. A series of some 30 photoelectric observations by Zaitseva (1968) well spaced over 400 days shows a variation of no more than 0^m1. The mean magnitude and color indices are $(V, B-V, U-B) = (7^m0, +0^m12, +0^m04)$ or $(6^m56, -0^m03, -0^m07)$ if the reddening for SU Aur used above is applicable to this star. The resulting color indices are normal for a main-sequence star of type B9 and if we apply the distance modulus derived from the group membership of SU Aur, $M_V = -0^m1$.

Bessell and Eggen (1972) have discussed the wide visual binary that contains the weak helium star (HR 5999), with strong lines of P II, and a shell star (HR 6000) of type A7 IV with Hα in emission. The shell star was found to vary with a visual range of one magnitude in about a one-month period and the light and polarization changes suggest that the variations are the result of obscuration by circumstellar dust clouds. It was concluded that the shell star, which at maximum is less than 0^m5 fainter than HR 6000, was prematurely evolving from the main sequence. However, subsequent discovery of several probable T Tauri, and other pre-main-sequence stars of later type in the vicinity of the pair now suggests that HR 6000 is one of the brightest known members of the class of Be and Ae stars discussed by Herbig.

HR 5999/6000, also known as the visual binary Dunlop 199, lies in an obvious absorption patch, as seen in Figure 15. This dark nebula, called L3 by The (1962), may be part of a larger cloud complex around η Lupi (HR 5848), which is a foreground object and a member of the Pleiades group (Table III). This larger cloud complex also contains the known T Tauri stars RY Lup and EX Lup and, perhaps, RU Lup. Observations of the stars marked 1, 2, 4, 5, and 6 on Figure 15 are listed in Table IX. Observations of No. 3 give $(V_E, B-V, U-B) = (9^m26, +0^m51, -0^m05)$ and unpublished spectra by M. S. Bessell

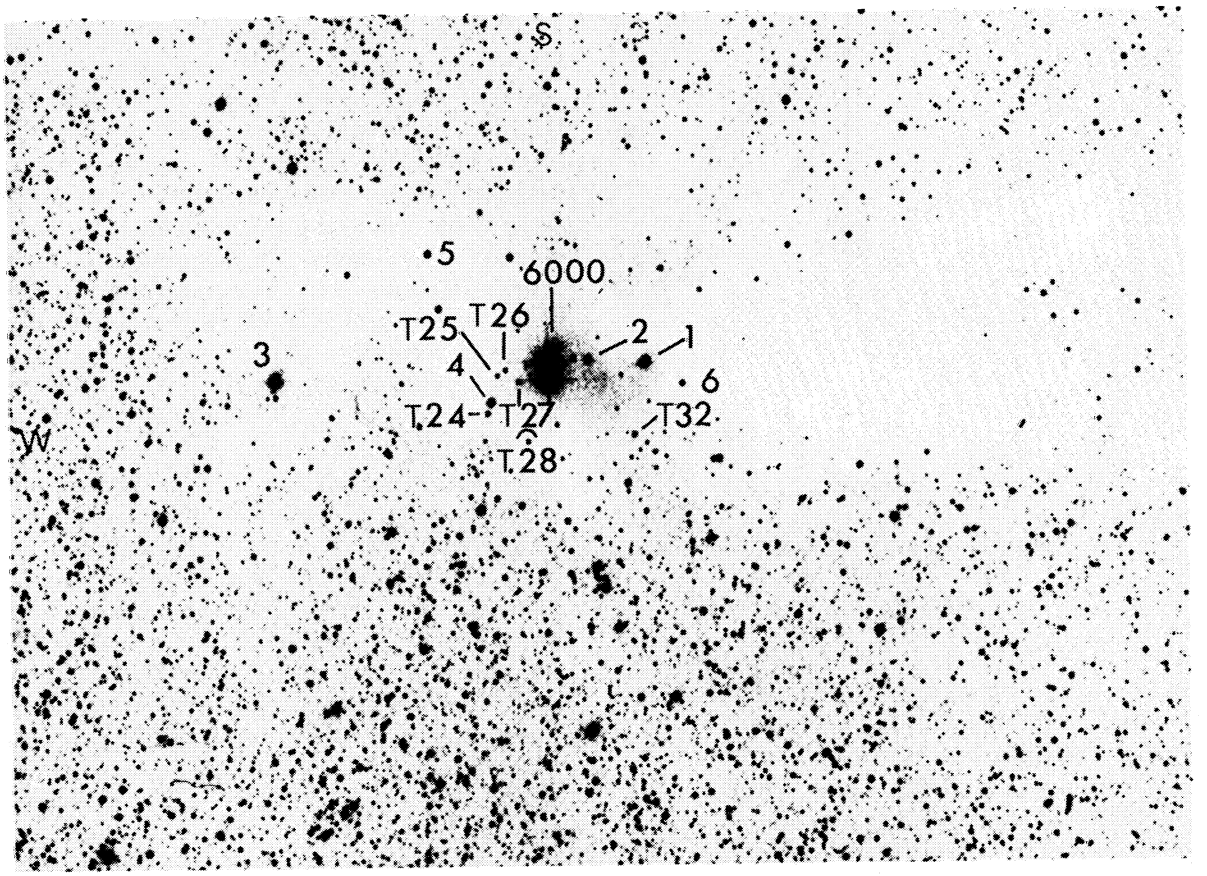

FIG. 15 — The region of HR 5999/6000. HR 5999 and HR 6000 are separated by 45".

TABLE IX

OBSERVATIONS OF FAINT STARS NEAR HR 5999/6000

	1			2			4			5			6		
	V_E	B-V	U-B	V_E	B-V	U-B	V_E	B-V	U-B	V_E	B-V	U-B	V_E	B-V	U-B
1974															
26 June	10.95	+1.04	+0.61	13.16	+1.47	+1.27	12.91	+1.50	+1.30	12.72	+1.21	+1.09	-	-	-
12 July	10.94	+1.02	+0.61	-	-	-	12.69	+1.19	+0.26	12.83	+1.22	+1.07	-	-	-
16 July	10.93	+1.02	+0.61	13.12	+1.45	+1.25	12.49	+1.17	+0.33	12.82	+1.22	+1.01	14.98	+1.48	+0.75
18 July	10.93	+1.01	+0.61	13.10	+1.45	+1.30	12.71	+1.17	0.00	12.79	+1.21	+1.03	14.80	+1.06	-0.39
21 July	10.94	+1.05	+0.62	13.13	+1.46	+1.31	12.77	+1.30	+0.485	12.80	+1.25	+1.04	14.90	+1.34	+0.29
23 July	10.91	+1.03	+0.59	13.14	+1.48	+1.28	12.69	+1.26	+0.38	12.72	+1.21	+1.10	14.89	+1.37	+0.26
24 July	10.95	+1.04	+0.63	13.17	+1.46	-	12.51	+1.29	+0.58	12.72	+1.25	+1.08	14.85	+1.24	-0.24
28 July	10.94	+1.03	+0.60	-	-	-	12.69	+1.31	+0.86	-	-	-	14.96	+1.46	+0.45
9 Aug	10.92	+1.03	+0.59	13.13	+1.46	+1.26	12.70	+1.34	+0.92	13.06	+1.24	+1.06	14.83	+1.23	-0.04
12 Aug	-	-	-	-	-	-	12.49	+1.23	+0.86	-	-	-	14.61	+1.12	-0.32
Means	10.93	+1.03	+0.61	13.14	+1.46	+1.27		VAR		12.8V?	+1.225	+1.06		VAR	

	R	R-I	R	R-I	R	R-I	R	R-I	R	R-I
27 June	10.46	+0.42	12.07	+0.865	12.14	+0.75	-	-	-	-
13 July	10.40	+0.42	12.03	+0.84	-	-	-	-	13.36	+1.22
19 July	10.40	+0.42	12.02	+0.84	11.54	+0.71	12.05	+0.535	13.41	+1.24
22 July	10.45	+0.425	12.00	+0.83	11.99	+0.765	12.07	+0.525	13.28	+1.13
11 Aug	-	-	12.06	+0.84	11.63	+0.705	-	-	13.36	+1.24
13 Aug	-	-	-	-	11.35	+0.625	-	-	13.30	+1.19
Means	10.43	+0.42	12.04	+0.84		VAR	12.06	+0.53		VAR

show it to be a subdwarf; HD 144477 (F8) with $\mu = 0''.07$. A faint companion to HR 5999, sometimes called See 265B, is 16″ distant in position angle 300°. Four observations with the 40-inch reflector in excellent seeing give (V_E, $B-V$, $U-B$) = ($12^m.55$, $+1^m.20$:, $+1^m.2$:) and (R, $R-I$) = ($11^m.60$, $+0^m.805$). Because of the proximity to the bright, blue star HR 5999 the *UBV* observations, and especially the value of ($U-B$), are uncertain but in (R, I) there should be little or no effect of contamination. HR 6000 is also a close double, Rossiter 3930, but the companion is near 12^m with a separation of only 1″.

Stars nos. 4 and 6 in Table IX are definitely variable and are almost certainly T Tauri objects. No. 4 is probably also the Hα emission star, no. 36, found by Stock and Wroblewski 1971, Table IVg); star no. 6 is no. 37 in the same reference. The (1962, Table III) found no emission in the present no. 4 but the present no. 6 is his no. 35 to which he assigns a type of M2. The also found Hα emission in a close companion to no. 4, which is labeled by his no. T24 in the present Figure 15. A single observation gives (R, $R-I$) = ($14^m.15$, $+1^m.235$). Five additional Hα emission objects found by The, T 24, T 25, T 27, T 28, and T 32, are also labeled in Figure 15, but observations of these stars are not completed. The variation for nos. 4 and 6 seen in Table IX are typical of T Tau stars (e.g., Mendoza 1968), with larger variations in B, and especially U, than in V.

The nonvariable (and non-Hα) stars in Table IX, nos. 1, 2, and 5, are shown as open circles in the ($R-I$, $U-B$) plane of Figure 16 where relations for Hyades giants (Eggen 1974*e*, Table III) and dwarfs (Eggen 1971*b*, Table 3) are shown as continuous curves. The plus sign indicates the faint companion to HR 5999, discussed above. Omitting the latter star because of the uncertainty in ($U-B$), the other objects are very probably dwarfs with the reddest (no. 2) showing a reddening of $E(R-I) = +0^m.07$ ($E(B-V) = +0.10$) and $E(R-I)$ is near $+0.2$ for the other two. Bessell and Eggen (1972) found $E(B-V) = +0^m.06$ for HR 5999.

The proper motion of HR 5999/6000 on the system used here is (μ_α, μ_δ) = ($-0''.008$, $-0''.024$) and $\rho = -2$ km sec^{-1}, giving $V_0 - M_V = 7^m.0$ for membership in the Pleiades group with (U, V, W) = ($+7$, -25, -14) km sec^{-1}. This value supersedes the $7^m.4$ given by Bessell and Eggen and based on a proper motion in the N 30 system without precessional corrections. The luminosity of HR 5999 is then $M_V = -0^m.6$, with ($B-V$, $U-B)_0$ = ($-0^m.13$, $-0^m.46$) (Bessell and Eggen 1972) and, at maximum light, HR 6000 has $M_V = -0^m.2$ with ($+0^m.225$, $+0^m.21$). Earlier observations of HR 6000 published by Bessell and Eggen have been supplemented with those in Table X. The light and color curves published previously (Bessell and Eggen 1972, Figs. 1 and 2 where "JD 2440000" should be added to the captions) demonstrated the quasi-periodic nature of the light variation for HR 6000 and, together with the polarization observations and the spectra, led to the conclusion that circumstellar dust clouds are being formed and dissipated. The new observations are in accordance with this conclusion. Previously the star was observed at fainter than visual magnitude 8 and the first observations in Table X were made when the light was rapidly increasing from a similar minimum. Representative 1973 and 1974 observations are shown in Figure 17.

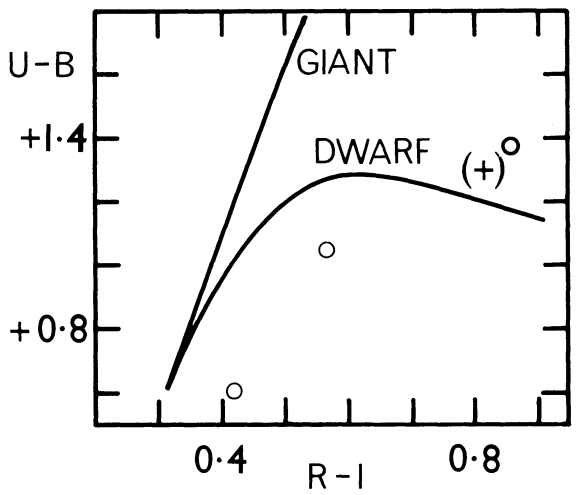

FIG. 16 — The nonvariable stars near HR 5999/6000 in the ($U-B$,$R-I$) plane. The plus sign indicates See 265b.

To overcome the difficulty in explaining the large difference between the "nuclear" age derived for, say, the Pleiades cluster from the brightest evolved stars and the "contraction" age derived from the fact that M-type stars have reached the main sequence, Herbig (1962) has suggested that two types of star formation should be considered. He supposes that stars

TABLE X

NEW OBSERVATIONS OF HR 6000

JD 244	V_E	B-V	U-B	R	R-I
1784	$7^m.87$	$+0^m.435$	$+0^m.275$		
1785				$7^m.57$	$+0^m.22$
1786	7.48	+0.39	+0.265		
1793	7.26	+0.37	+0.23		
1794				7.04	+0.18
1795	7.21	+0.34	+0.185		
1810	7.16	-	-		
1811	7.06	-	-		
1821				7.07	+0.195
1822	7.16	+0.36	+0.20		
1824	7.22	+0.38	+0.175		
1825				7.12	+0.18
1866	7.16	+0.36	+0.19		
1867	7.07	+0.34	+0.23		
1886				6.77	+0.145
1887	6.94	+0.34	+0.30:		
1891	6.88	+0.33	+0.29		
1892				6.71	+0.145
1893				6.78	+0.135
1908	7.03	+0.345	+0.245		
1924	6.99	+0.325	+0.275		
1925				6.88	+0.145
1926	7.03	+0.305	+0.22		
1940	7.61	+0.47	+0.305		
1941	7.45	+0.395	+0.27		
1942				7.20	+0.205
1943	7.26	+0.385	+0.255		
1944				7.18	+0.19
2225	7.14	+0.36	+0.265		
2226				7.12	+0.16
2241	7.25	+0.345	+0.28		
2242				7.21	+0.16
2245	7.26	+0.345	+0.265		
2247	7.20	+0.335	+0.23		
2248				6.99	+0.155
2250	7.01	+0.335	+0.225		
2251				6.91	+0.15
2252	6.94	+0.32	+0.22		
2253	6.94	+0.32	+0.20		
2255	6.95	+0.32	+0.24		
2257	7.00	+0.32	+0.22		
2269	6.91	+0.31	+0.205		
2271				6.83	+0.145
2272	6.97	+0.31	+0.21		
2273				6.89	+0.165

of intermediate and low mass can be formed only under special circumstances in dense clouds containing much dust and having a very low temperature and turbulence. Over long periods of time the medium- and low-luminosity stars are formed in these clouds but when an O or early B-type star nears the main sequence all star formation halts in the resulting H II region because of the evaporation of the dust and the high kinetic and turbulent activity that immediately ensues. Those low- and medium-mass stars that have become sufficiently advanced in the process of contraction and have effectively become isolated from the nebular material may not be affected by the activity accompanying the advent of the high-mass star. This attractive hypothesis has the additional advantage that it may explain why the main sequences of some galactic clusters are truncated, for the timing of the advent of the high-mass star will dictate the luminosity function of the cluster and if this event is early enough in the history of the dark cloud only a group of early-type stars will result, forming the many known trapezium-like, multiple systems. The attractiveness of this hypothesis is enhanced by the presence in many very young clusters of a distinct gap in the stellar distribution near the main sequence at $M_V = 0^m$ to -1^m. Such a gap exists in the Pleiades cluster (e.g., Eggen 1965, Fig. 13) with the shell star, Pleione, falling in the gap. Shell stars in the α Per and NGC 2516 clusters (Eggen 1972) fall in similar gaps for these clusters and there is a strong inference that they represent the top of the main sequence for the medium- and low-mass stars that formed prior to the event that produced the half-dozen early B-type stars brighter than M_V near -1^m in all three clusters. Walker's (1956) photoelectric observations of members of the very young cluster NGC 2264

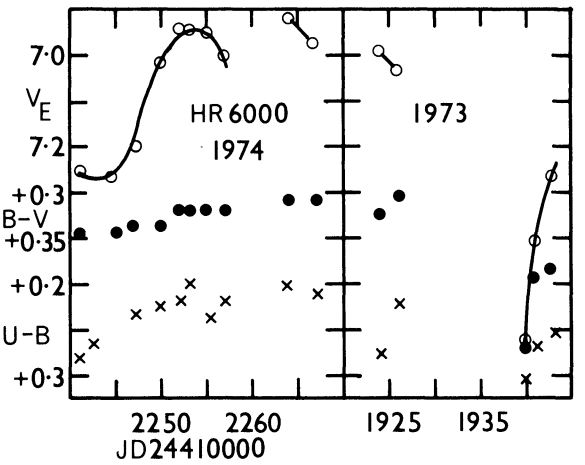

FIG. 17 — Light and color curves for HR 6000.

are shown in Figure 18 after correcting for a reddening of $E(B-V) = +0^m08$ and a modulus of $V_0 - M_V = 9^m6$ (Eggen 1974*a*). A few known T Tauri variables in this cluster are indicated by slashed circles. The gap near $M_V = 0^m$ is clearly defined. The variable and nonvariable stars in the vicinity of HR 5999/6000, discussed above, are also shown in the figure as are the pair AB Aur and SU Aur. It is of interest to compare the pair HR 5999/6000 with Walker nos. 109 and 100 in the cluster NGC 2264 as this latter pair, which is ADS 5322FG, would be a prominent feature of the cluster if the stars above the gap at M_V near -1^m were removed. Star no. 109 is, like HR 5999, a peculiar object with a variable spectrum and, perhaps, shell characteristics (Bernacca and Ciatti 1972). Star no. 100, which is of type A2 IV (Walker 1956) is not unlike HR 6000, except that no variation has been detected

	M_V	$(B-V)_0$	$(U-B)_0$
HR 5999	-0^m6	-0^m13	-0^m46
No. 109	−0 .7	−0 .18	−0 .62
No. 100	+0 .15	+0 .06	+0 .01
HR 6000	-0^m2	$+0^m225$	$+0^m21$.

Helium-weak (i.e., peculiar A-type) stars with luminosities similar to star no. 109 and HR 5999 are known in several young clusters and it seems reasonable to suppose that these peculiarities are the result of a magnetic accretion process (e.g., Havnes 1974) operating in the thin "cocoon" nebulae, or circumstellar dust shells that the contracting stars of medium mass carry to the main sequence (e.g., Herbig 1970).

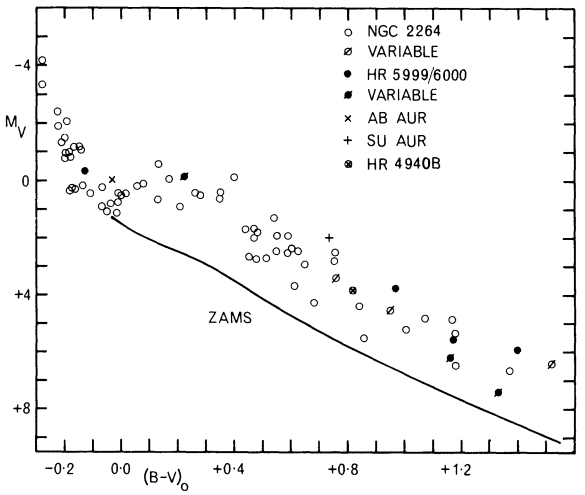

FIG. 18 — Pre-main-sequence stars in the $(M_V, B-V)$ plane.

The scale of star production in the local association appears to vary from the large number of completed A- to M-type main-sequence objects in the populous clusters like the Pleiades and NGC 2516 and the numerous pre-main-sequence stars now forming in the Taurus-Aurigae dark cloud, to the relatively small-scale operation now producing stars in the region around HR 5999/6000. Other apparently isolated regions of small-scale production, which will be discussed in detail elsewhere, include a region in Chamaeleon, containing several T Tauri stars (e.g., Henize 1963; Henize and Mendoza 1973), a similar region in Lupus (Henize 1954) and a small group of stars near the T Tauri variable BM Andromedae (Aveni and Hunter 1969). A visual inspection of all these small regions shows that an undoubtedly significant feature of the stellar distribution is the domination by a pair of nearly equal, late B-type stars similar to HR 5999/6000: in the Chamaeleon region it is HD 97048 and HD 97300, a very wide pair with common proper motion and radial velocity (M. S. Bessell, unpublished) and spectral types of A0 eα and A0 V, respectively (Henize 1963); in the Lupus region, which is only some 3° from HR 5999/6000, it is the wide, common proper-motion pair HD 140817 (B9, $V = 6^m86$) and HD 140840 (B9, $V = 7^m38$); and the region of BM And is dominated by the common proper-motion pair HD 222086 and HD 222142 (B9) (Aveni and Hunter 1969, Plate IIb). One of the most interesting southern regions, covering NGC 6726/7 and NGC 6729 and including T Coronae Austrinae, R. Coronae Austriane, and TY Coronae Austrinae, is near the wide, common proper-motion pair HR 7169 (B8) and HR 7170 (B8). Both stars are spectroscopic binaries, with the brighter showing double lines, and are very probably at the same distance as the T Tauri objects. Perhaps the smallest regions of star production are now represented by the pre-main sequence companions to some isolated members of the Pleiades group of which the best example may be the close (12″) companion of HR 4940, that Thackeray (1966) classifies as K0 Ve. Andrews and Thackeray (1973) give $V = 10^m8$ and $(B-V) = +0^m82$ but the closeness of the brighter star makes this result uncertain. Observations with the 40-inch reflector in excellent

seeing give $(R, R-I) = (10^m49, +0^m34)$ and we would therefore expect $(V-R)$ to be 0^m4 (Eggen 1971*b*, Table 3), which indicates that the observed value of V is correct within 0^m1. The observed value of $(R-I)$ leads to a value of $(B-V) = +0^m9$ for a star of solar composition, which may indicate that the observed value of $+0^m8$ is slightly contaminated in B by the nearby bright star. A value of $(B-V) = +0^m85$ has been adopted and the star is shown in Figure 18 as a circled cross at a luminosity derived from the modulus of 6^m85 (Eggen 1974*b*, Table 11).

VII. Spectral Classification

Spectral types are not listed for many of the stars discussed here, partly because there are so many possible classifications available in the literature for many of the objects but also because the values of $([u-b], \beta)$ give a more quantitative estimate of temperature and luminosity, at least for stars later than B0. Using the few revised standards on the MK system published by Morgan and Keenan (1973, Table 1), the positions of various spectral and luminosity classes in the $([u-b], \beta)$ plane are shown in Figure 19. In some respects the spectral types may be most important when they indicate an incorrect temperature or luminosity. Examples of this are the helium-weak stars (e.g., Garrison 1967) which are often classified B7–9 III or IV on the MK system but have photometric parameters characteristic of B4–6. Two known examples of this phenomenon are the first two entries in Table XI, which also contains an additional eight candidates selected on the basis of the spectral type derived from the photometric parameters. It is of course necessary to eliminate objects with hydrogen emission before the photometric parameters used here can be trusted to isolate helium-weak stars.

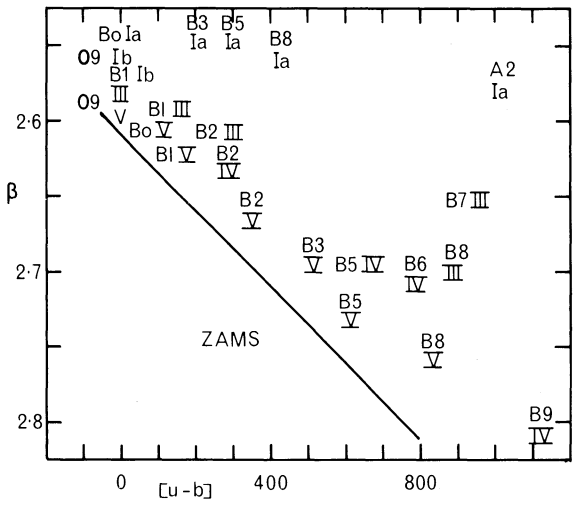

FIG. 19 — Standard spectral types and luminosity classes in the $([u-b], \beta)$ plane.

VIII. Summary

Intermediate-band indices are used to derive luminosities for some 500 early-type stars (M_V brighter than -1^m) with well-determined proper motions and radial velocities. Space motion vectors (U, V, W) and galactic coordinates ($X, Y,$

TABLE XI

POSSIBLE He WEAK STARS

HR	[u-b] (0.001)	β	Sp. Pt.	Sp. MK
280*	687	2.660	b6 III	B8 III
1063*	587	2.700	b4 V	B8 III
113*	764	2.689	b6 IV	B9 III
1441*	603	2.720	b5 V	B9 III
2497	713	2.716	b6 V	B9 III
2676	744	2.705	b6 IV	B9.5 III
3571	772	2.701	b6 IV	B8 II
7129*	489	2.683	b3 V	B9 III
8478*	560:	2.722	b5 V	B8 III
8535	605	2.694	b5 IV	B8 III-IV

Notes to Table XI

280 α Scl, known He weak star.

1063 Known He weak star, member of α Per cluster (Pleiades group).

113 Member of Pleiades group.

1441 Not included in present discussion because $M_V = -0^m75$. $(\mu_\alpha, \mu_\delta) = (+0.001, -0.013)$, $\rho = +15.2$ km/sec and (U,V,W) = (+6,-13,-12) km/sec.

7129 Member of Pleiades group and near the group of T Tau stars in CrA. Present observations indicate a variation of 0^m1 in V_E. [Later note: Balona and Martin (1974) have found the helium lines to be variable in a period of 3.7 days.]

8478 The value of [u-b] is poorly determined and the star is not included in the present discussion. However, the value of $(U-B)_0 = -0^m56$ supports the earlier classification of b5.

Z) are computed for these stars and are the basis of the following results.

1. The local association (Pleiades group) stars are easily isolated on the basis of the unique values of $V = -25$ km sec^{-1}.

2. About one-third of the early-type stars belong to the local association.

3. The local association members are mainly concentrated in the Sco-Cen region in the Southern Hemisphere — including the cluster NGC 2516 — and the Cas-Tau region in the north — including the Pleiades and α Persei clusters.

4. The local association includes several groups of stars on the edges of dark clouds (T associations) that range in size from that in Taurus to the small absorption patch in Lupus near HR 5999/6000.

5. The ages of stars in the local association range from that of the cluster NGC 2287 to pre-main-sequence stars in the associated dark clouds.

6. Some 50 stars with aberrant velocity vectors may be members of the old-disk (blue stragglers) or even the halo (suprahorizontal-branch stars) populations.

REFERENCES

Abt, H. A., and Biggs, E. S. 1972, *Bibliography of Stellar Radial Velocities*, (Tucson: Kitt Peak National Observatory).

Abt, H. A., Jeffers, H. M., Gibson, J., and Sandage, A. R. 1962, *Ap. J.* **135**, 429.

Andrews, P. J. 1968, *Mem. R.A.S.* **72**, 35.

Andrews, P. J., and Thackeray, A. D. 1973, *M.N.R.A.S.* **165**, 1.

Aveni, A. F., and Hunter, J. H. 1969, *A.J.* **74**, 1021.

Balona, L., and Martin, W. L. 1974, *M.N.R.A.S.* **166**, 35P.

Bernacca, P. L., and Ciatti, F. 1972, *Astr. and Ap.* **19**, 482.

Bessell, M. S., and Eggen, O. J. 1972, *Ap. J.* **177**, 209.

Blaauw, A. 1961, *Astr. Inst. Netherlands* **15**, 265.

Buscombe, W. 1965, *M.N.R.A.S.* **129**, 411.

Cousins, A. W. J., Eggen, O. J., and Stoy, R. H. 1961, *Roy. Obs. Bull.* No. 25.

Cowley, A., Cowley, C., Jaschek, M., and Jaschek, C. 1969, *A.J.* **79**, 375.

Crawford, D. L., and Barnes, J. V. 1970, *A.J.* **75**, 952.

Crawford, D. L., Barnes, J. V., and Golson, J. C. 1970, *A.J.* **75**, 264.

—— *ibid.* **76**, 1058.

Crawford, D. L., Barnes, J. V., and Warren, W. H. 1974, *A.J.* **79**, 623.

Crawford, D. L., Barnes, J. V., Golson, J. C., and Hube, D. P. 1973, *A.J.* **78**, 731.

Eggen, O. J. 1965, *Annual Rev. of Astr. and Astrophysics* **3**, 235.

—— 1970*a*, *Vistas in Astronomy* **12**, 367.

—— 1970*b*, *Ap. J.* **161**, 159.

—— 1971*a*, *ibid.* **163**, 313.

—— 1971*b*, *Ap. J. Suppl.* **22**, 389.

—— 1972, *Ap. J.* **173**, 63.

—— 1974*a*, *Pub. A.S.P.* **86**, 960.

—— 1974*b*, *Ap. J.* **188**, 59.

—— 1974*c*, *Pub. A.S.P.* **86**, 241.

—— 1974*d*, *ibid.* **86**, 162.

—— 1974*e*, *ibid.* **86**, 129.

Fredrick, L. W. 1956, *A.J.* **61**, 437.

Garmany, C. D. 1973, *A.J.* **78**, 185.

Garrison, R. F. 1967, *Ap. J.* **147**, 1003.

Graham, J. 1967, *M.N.R.A.S.* **135**, 377.

Grant, G. 1959, *Ap. J.* **129**, 78.

Havnes, O. 1974, *Astr. and Ap.* **32**, 161.

Heinze, K. G. 1954, *Ap. J.* **119**, 459.

—— 1963, *A. J.* **68**, 280.

Henize, K. G., and Mendoza III, E. E. 1973, *Ap. J.* **180**, 115.

Herbig, G. H. 1960, *Ap. J. Suppl.* **4**, 337.

—— 1962, *Adv. in Astr. and Astrophysics* **1**, 47.

—— 1970, *Mem. Roy. Soc. Sc. Liège* **19**.

—— 1973, *Ap. J.* **182**, 129.

Herbig, G. H., and Rao, K. 1972, *Ap. J.* **174**, 401.

Klinglesmith, D. A. 1972, *Ap. J.* **171**, 79.

Lesh, J. R. 1968, *Ap. J. Suppl.* **17**, 371.

—— 1972, *Astr. and Ap. Suppl.* **5**, 129.

Lyngå, G. 1968, *Ark. f. Astr.* **3**, 65.

Mendoza III, E. E. 1968, *Ap. J.* **151**, 977.

Morgan, W. W., and Keenan, P. C. 1973, *Annual Rev. of Astr. and Astrophysics* **11**, 29.

Osawa, K. 1959, *Ap. J.* **130**, 159.

Perry, C. L., and Hill, G. 1969, *A.J.* **74**, 899.

Racine, R. 1968, *A.J.* **73**, 233.

Roark, T. P. 1971, *A.J.* **76**, 634.

Ruprecht, S. 1966, *I.A.U. Trans.* **12b**, 348.

Schmidt-Kaler, T. 1961, *Zs. f. Ap.* **53**, 28.

Stock, J., and Wroblewski, H. 1971, *Pub. Dept. of Astr. University of Chile* **2** (No. 3).

Stokes, N. R. 1972*a*, *M.N.R.A.S.* **159**, 165.

—— 1972*b*, *ibid.* **160**, 155.

Stothers, R., and Frogel, J. A. 1974, *A.J.* **79**, 456.

Strömgren, B. 1966, *Annual Rev. of Astr. and Astrophysics* **4**, 433.

Thackeray, A. D. 1966, *Mem. R.A.S.* **70**, 33.

The, Pik-Sin 1962, *Contr. Bosscha Obs.* No. 15.

Walker, M. F. 1956, *Ap. J. Suppl.* **2**, 365.

Zaitseva, G. V. 1968, *Peremennye Zvedy* **16**, 435.

Zinn, R. J., Newell, E. B., and Gibson, J. B. 1972, *Astr. and Ap.* **18**, 390.